Hochschule für Angewandte Wissenschaften Hamburg
Hamburg University of Applied Sciences

Master Thesis

Radosław Sierocki

Implementation of the action plane fracture criteria of Puck into the Finite Element code Abaqus

Faculty of Engineering and Computer Science
Department of Computer Science

Hamburg University of Applied Sciences

Faculty of Engineering and Computer Science

Department of Automotive and Aeronautical Engineering

Berliner Tor 9

20099 Hamburg

Germany

Author: Radosław Sierocki

Date: 23.08.2016

Supervisor: Prof. Dr.-Ing. Dipl. -Kfm. Markus Linke

Co-supervisor: Prof. Dr. -Ing. Jens Baaran

Faculty of Engineering and Computer Science
Department of Computer Science

Abstract

The topic of this Master's thesis is the implementation of the action plane fracture criteria of Puck into the Abaqus (3DS Dassault Systems, Paris, France) environment. The proper code will be developed in Fortran code. The necessity of using this criterion follows that in Finite Element codes the strength of fibre-reinforced plastic is typically computed based on an analytical function describing the yield surface. Therefore, it cannot be distinguished between different failure modes. The Puck's failure criterion singles out the fibre failure and inter-fibre failure. Even though Abaqus options include Hashin theory, which also distinguish IFF and FF, Hashin didn't take into account the fracture plane and in Abaqus Hashin's criteria is only available for 2D model. That is why this criterion is one of the best failure criteria for fibre-reinforced plastic available today.

The Puck's failure criterion code will be done in an implicit way. It is important to check whether this code is working properly in cooperation with Abaqus software. There is a need of validation this implementation. The first step to achieve it, is to prepare some example based on literature and calculate them using Compositor composite's calculator (program prepared and developed by Instutut für Kunsttoffverarbeitung, RWTH Aachen). These calculations will serve in the next step of this thesis, when this results will be checked with the one achieved with Abaqus software and implemented code. To obtain the validation of action plane fracture criteria of Puck, results from numerical calculations must be similar with experiments ones.

Ensuring that the code works correctly and it provides acceptable results, action plane fracture criteria of Puck will be used in modeling and calculating degradation process in composite structure. By using action plane fracture criteria of Puck there is a wish to obtain a properly defined model and thanks to that receive correct results for numerical calculations.

Thanks to this work we achieved a subroutine that can allow us to calculate a 3-dimensional model of a lamina. It is important, because now we can model more complex of laminate structure, not only 2-dimensional models, which in many cases are not sufficient. The implementation will improve researches about degradation processes in laminate structures, which was not available before.

Table of contents

Abstract 1
Table of figures 3
Table of datas 4
Abbreviations 5
Used symbols and their units 5
1. Introduction 1
1.1. Motivation 1
1.2. Tasks 1
1.3. Structure of the thesis 2
2. Action plane fracture criteria of Puck 3
2.1. General information 3
2.2. Fibre fracture conditions 5
2.3. Inter-fibre fracture 6
2.3.1. Action planes and fracture planes 6
2.3.2. Fracture modes 8
2.3.3. Action plane stresses 11
2.4. Material law 14
2.5. Weakening factor 15
2.6. Material degradation 16
3. Degradation procedure 19
4. Experimental data and Compositor calculations 28
4.1. Degradation of 3-layer lamina with 0°/90°/0° layers 28
4.2. Degradation of 3-layer lamina with -45°/90°/-45° layers 33
5. Abaqus Cae standard 37
5.1. 2D state of stress 37
5.2. 3D state of stress 38
6. Comparison between Abaqus and Compositor results 40
6.1. Abaqus results for example from section 4-1 40
6.2. Abaqus results for example from section 4-2 46
6.3. Abaqus results for example from section 4-2 for 3-dimensional state of stress 48
7. Summary 54
8. Conclusion 55
References 56
Appendixes 56

Declaration 57

Table of figures

Figure 2-1 Basic stressing of a lamina, [Lit.2.] p. 35. 4
Figure 2-2 Puck's fracture cigar, [Lit.1.], p. 46 5
Figure 2-3 Three dimensional stressing in local COS and laminate COS, [Lit.2.], p. 12. 6
Figure 2-4 Basic stressings and their action planes, [Lit.1.], Page 48. 7
Figure 2-5 Fracture planes, [Lit.1.], Page 49 8
Figure 2-6 Shear stresses on action plane, [Lit.1.], Page 50 9
Figure 2-7 Vizualization of stress factor, [Lit.1.], Page 51 10
Figure 2-8 Action plane stresses, [Lit.2.], Page 44 12
Figure 3-1 Solution depended variables settings 20
Figure 3-2 Solution process 21
Figure 3-3 Graphical interpretation of TIME(2), TIME(1) and DTIME variables 22
Figure 3-4 Material constants settings 23
Figure 3-5 Solution finding process 26
Figure 4-1 Sketch of loading and bundary conditions 29
Figure 4-2 Material constants of 90 degree layer [see Ap.2] 30
Figure 4-3 Applied load (cp. Appendix.2.) 30
Figure 4-4 State of strains in the 90 degree layer (cp. Appendix.2.) 31
Figure 4-5 State of stress in the 90 degree layer (cp. Appendix.2.) 32
Figure 4-6 State of stress in the 0 degree layer (cp. Appendix.2.) 32
Figure 4-7 Material constants of 90 degree layer (cp. Appendix.3.) 33
Figure 4-8 Material constants of -45 degree layer (cp. Appendix.3.) 34
Figure 4-9 Applied load (cp. Appendix.3.) 34
Figure 4-10 State of stress in the 90 degree layer (cp. Appendix.3.) 35
Figure 4-11 State of stress in the 0 -45 degree layae (cp. Appendix.3.) 36
Figure 5-1 2D model and boundary conditions 37
Figure 5-2 0XZ boundaray conditions for 3D model 38
Figure 6-1 IFF for 90 degree layer in the 0/90/0 layup 41
Figure 6-2 Sigma_1 stress for 90 degree layer in the 0/90/0 layup 42
Figure 6-3 Sigma_2 stress for 90 degree layer in the 0/90/0 layup 43
Figure 6-4 Young's modulus for 90 degree layer in the 0/90/0 layup 44
Figure 6-5 Shear modulus for 90 degree layer in the 0/90/0 layup 45
Figure 6-6 Sigma_2 stresess in the 45/90/45 lamina 46

Figure 6-7 IFF in the 45/90/45 lamina 47
Figure 6-8 IFF for the end step with the possible contraction in the Z-direction 49
Figure 6-9 Sigma_1 for the end step with the possible contraction in the Z-direction 50
Figure 6-10 Sigma_2 for the end step with the possible contraction in the Z-direction 51
Figure 6-11 Young's modulus for the end step with the possible contraction in the Z-direction 52
Figure 6-12 Shear modulus for the end step with the possible contraction in the Z-direction 53

Table of datas

Table 2-1 Slope parameters, [Lit.1.], p. 57 13
Table 2-2 Different modes and their stresses, [Lit.1.], Page 59 14
Table 6-1 Comparison of IFF in 90 degree layer for 0/90/0 layup 41
Table 6-2 Comparison of sigma_1 stress in 90 degree layer in 0/90/0 layup 42
Table 6-3 Comparison of sigma_2 stress in 90 degree layer in 0/90/0 layup 43
Table 6-4 Comparison of E_2 in 90 degree layer in 0/90/0 layup 44
Table 6-5 Comparison of G_12 in 90 degree layer in 0/90/0 layup 45
Table 6-6 IFF comparison between two Abaqus models 48
Table 6-7 Sigma_1 comparison between two Abaqus models 49
Table 6-8 Sigma_2 comparison between two Abaqus models 50
Table 6-9 Young's modulus comparison between two Abaqus models 51
Table 6-10 Shear modulus comparison between two Abaqus models 52

Abbreviations

IFF - inter-fiber fracture

FF- fibre fracture

FEA- Finite Element Method

COS- coordinate system

Used symbols and their units

$\sigma_1, \sigma_2, \sigma_3$ [MPA] – normal stresses in the material COS

σ_{1f} [MPa] – fibre directions stress

$\tau_{12}, \tau_{13}, \tau_{23}$ [MPa] – shear stresses in the material COS

$\sigma_x, \sigma_y, \sigma_z$ [MPA] – normal stresses in the global COS

$\tau_{yz}, \tau_{xz}, \tau_{xy}$ [MPa] – shear stresses in the global COS

$\sigma_{\parallel}^{t,c}$ [MPa] – normal stresses parallel to fibre direction (t for tension, c for compression)

$\sigma_{\perp}^{t,c}$ [MPa] – normal stresses perpendicular to fibre direction

$\tau_{\perp\parallel}$ [MPa] – in – plane shear stresses

$\tau_{\perp\perp}$ [MPa] – through – thickness shear stresses

σ_n [MPa] – normal stress in the action plane

τ_{n1} [MPa] – shear stress in the action plane, parallel to fibre direction

τ_{nt} [MPa] – shear stress in the action plane, perpendicular to fibre direction

θ [°] – the angle of the action plane

θ_{fp} [°] – the angle of the fracture plane

ψ [°] – the angle between τ_{n1} and τ_{nt} in the action plane

η_{w1} [–] – weakening factor

η_R [–] – residual stiffness fracture

η_{RE} [–] – residual stiffness fracture for Young's modulus

η_R [–] – residual stiffness fracture for shear modulus

$\upsilon_{12}, \upsilon_{21}, \upsilon_{13}, \upsilon_{31}, \upsilon_{23}, \upsilon_{32}$ [–] – Poisson's numbers

a, ζ [–] – equation constants for residual stiffness fraction

$f_{E\,FF}$, Fb $[-]$ – fibre fracture

$f_{E\,IFF}$, Zfb $[-]$ – inter – fibre fracture

$f_{E0}[-]$ – inter – fibre fracture with no weakening effect

$f_{E1}[-]$ – inter – fibre fracture with including weakening effect

E_1, E_2, E_3 [MPa] – Young's modulus, material COS indexing

G_{12}, G_{13}, G_{23} [MPa] – shear modulus, material COS indexing

$E_{\parallel}, E_{\perp}$ [MPa] – Young's modulus, direction of acting indexing

$G_{\perp\parallel}$ [MPa] – shear modulus, direction of acting indexing

f_S $[-]$ – stretch factor

f_E $[-]$ – exposure factor

$R^c_{\parallel}, R^t_{\parallel}, R^c_{\perp}, R^t_{\perp}, R_{\perp\parallel}, R_{\perp\perp}$ [MPa] –
material strength resistances in reference to direction and kind of stress

R_{σ}, R_{τ} [MPa] – material strength resistances in reference to kind of stress

R^A [MPa] – strength resistance of the action plane

$p^t_{\perp\parallel}, p^c_{\perp\parallel}, p^t_{\perp\perp}, p^c_{\perp\perp}$ $[-]$ – slope parameters

1. Introduction

1.1. Motivation

The importance of efficiency is increasing more and more these days. It is no different in aircraft design where since many years engineers are trying to develop new materials for airplanes structures, which can decrease their weight. Steel and aluminium alloys are no more sufficient due to their mass and limited strength for lightweight constructions. That is why it leaded to use of fiber-reinforced plastics. Composites offer not only outstanding mechanical properties but also high potential for lightweight.

As always, every technology has some disadvantages. The main deficiency of using composites is not only the cost of manufacture them but also case of repair. This leads to increased weight. Due to this fact, it is often, that instead of repairing damaged structures, a whole part is replaced. Nevertheless, a new technology of fixing defects is providing these days. The idea of adhesive bonded scarf repairs, reinforced with high strength yarns, improves bonding characteristics (cp. [Lit. 2.]).

Even thought, the new approach is sensible reliable, there is a need to validate strength properties of such bonded joints. Among all available strength criterions for composites, action plane fracture criteria of Puck is the most suitable. The necessity of using this criterion follows that in Finite Element Method yarns are idealized based on classical laminate theory. Nevertheless, with the action plane fracture criteria of Puck we can obtain an improvement of the model.

Follow the fact that this process must be computerized and automated, there is a need to create a composite model for the yarn in Abaqus (3DS Dassault Systems, Paositeris, France) environment. However, options in Abaqus do not allow to model composite as three-dimensional solid element. An implementation of action plane fracture criteria of Puck into Abaqus allows to determined the proper model for yarn.

1.2. Tasks

The task of this thesis is to implement the action plane fracture criteria of Puck into Abaqus software and use it to provide a degradation process for a modeled lamina. To achieve it, a proper subroutine must be provided in a Fortran code. To check, whether it is working properly, results from numerical calculation must be compared with experimental data and also examples solved in Compositor (program prepared and developed by Instutut für Kunsttoffverarbeitung, RWTH Aachen). Compositor is an calculation spreadsheet, developed and destined to provided 2-dimensional model of lamina. It allows to calculate

actual state of stress on the basis of state of strain using classical laminate theory and on the basis of Puck's criteria, check whether fibre fracture and inter-fibre fracture occurs in modeled example of lamina.

1.3. Structure of the thesis

The thesis will be divided in two parts: theoretical and practical. In the theoretical part the action plane criteria of Puck will be introduced first. Then the material law of orthotropic material will be provided. As the last, the degradation process will be explained with introduction of proper subroutine that must be used in this process to properly model material behavior of lamina in each integration point.

In the practical part of this thesis the validation process of the action plane criteria of Puck will be discussed. To achieve the validation, two examples from literature of degradation process will be provided in Compositor calculation spreadsheet. These examples then will be compared with results achieved with Abaqus software with the usage of implemented Fortran subroutine code.

At the end a summary and conclusions will be presented. As the next step, the implemented action plane fracture criteria of Puck will be used in bended joints reinforced with yarns in the bending line.

2. Action plane fracture criteria of Puck

This chapter will shortly introduce essence of action plane fracture criteria of Puck in accordance with the Lit. 1 and the Lit 2. The main task of such criteria is to determine whether a load applied to the structure leads to fracture or not. It also allows us to achieve information about degradation process and how lamina would behave with different type of layup. This is possible thanks to complexity of this criteria, which is going to be described below.

2.1. General information

In fiber-reinforced laminas two different types of fracture can occur. It is distinguish between fibre fracture (FF) and inter-fibre fracture (IFF). The necessity of dividing procedure comes from the fact that FF and IFF have different influence on the load-carrying capacity of laminates. Briefly saying, IFF must be taken into account but under some certain circumstances can be acceptable. On the other hand, FF almost always means the loss of the load-carrying capacity of the laminate.

We can single out few main kinds of stresses that can appear in a loaded structure (cp. Fig. 2-1). These are compression-tension normal stresses and shear stresses. Furthermore we can distinguish compression-tension stresses on these which work parallel to the fibre direction $\sigma_{\parallel}^{t,c}$ and perpendicularly to the fibre direction $\sigma_{\parallel}^{t,c}$ ("t" for tension, "c" for compression). As well, we can divide shear stresses into these which work in plane parallel to fibre direction $\tau_{\perp\parallel}$ (in-plane shear stresses) and these which work in-plane perpendicular to fibre direction $\tau_{\perp\perp}$ (trough-thickness shear stresses).

While, fiber fracture mostly occurs when stresses are parallel to the fibre direction ($\sigma_{\parallel}$), for inter-fibre fracture the most important are streses $\sigma_{\perp}$ transverse to the fibre direction and shear stresses: in-plane shear stresses $\tau_{\perp\parallel}$ and trough-thickness shear stresses $\tau_{\perp\perp}$. To achieve best mechanical properties laminates should consist of several unidirectional plies with different fibre orientations. Therefore, different types of failure can occur, according to type of load (cp. Fig. 2-1]).

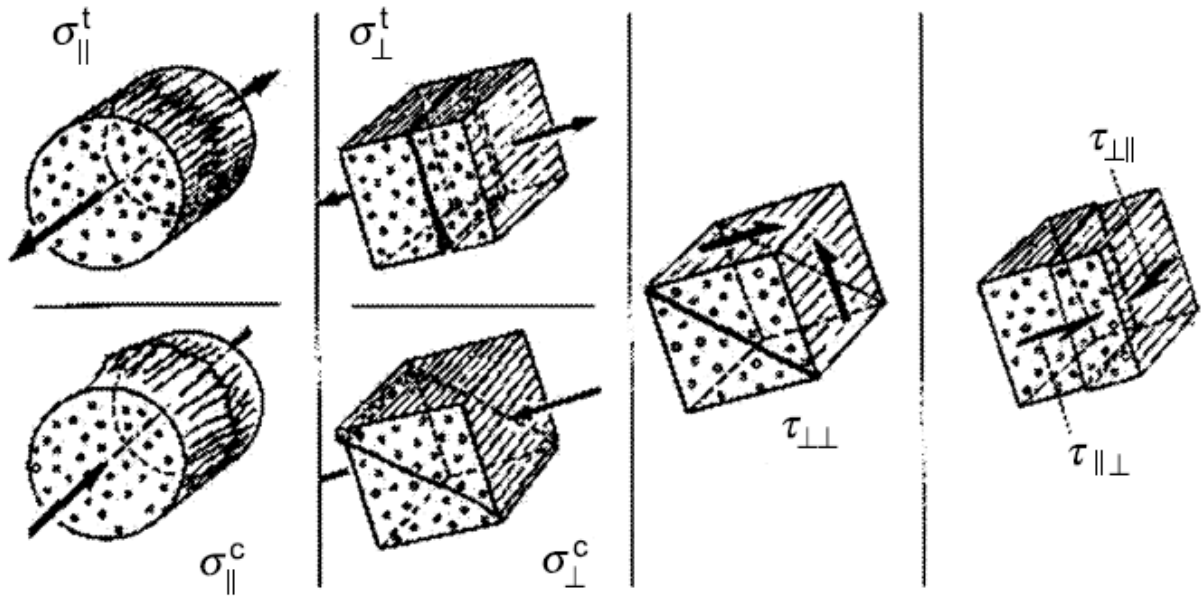

Figure 2-1 Basic stressing of a lamina, [Lit.2.] p. 35.

It is important to understand that plane fracture criteria of Puck, as well as other criterias, is a hypothesis. It means basing on only few known states of fracture, it gives an infinite number of possible states. These determined states of fracture are related to basic strengths. In the case of unidirectional lamina these are ones referred to applied tension and compression: $R_{\|}^{c}, R_{\|}^{t}, R_{\perp}^{c}, R_{\perp}^{t}$ and in-plane and out-of-plane shear: $R_{\perp\|}$, $R_{\perp\perp}$. Basic strengths are material constants, which define the material resistance to act of appropriate stresses. Indexes in their symbols are related to stresses they are referred to. These values can be for instance determined experimentally. Furthermore, the fracture criterion defines a closed surface in the six-dimensional stress space (σ_1,σ_2,σ_3,τ_{12},τ_{13},τ_{23}). This surface, in the best case, includes all available experimental specified strengths and predicts fractures at all other stress combinations. The Fig.2-2. shows the so called Puck's fracture cigar for a 2-dimensional state of stress (σ_1,σ_2,τ_{12})

This surface is the representation stress state of three stresses (σ_1,σ_2,τ_{12}) . Fb is the abbrevation for sub-surface for fibre-fracture and Zfb for sub-surface for inter-fibre fracture.

For 3-dimensional state of stress the strength criteria is formulated as function of stresses and strength resistance parameters (cp. [Lit.2.], p. 36).

$$\mathrm{F}(\sigma_1, \sigma_2, \sigma_3, \tau_{23}, \tau_{31}, \tau_{21}, R_\sigma, R_\tau) \lesseqgtr 1 \qquad [2.1]$$

If equation [2.1] results in F=1, it is termed the fracture condition. In other words, when a value F=1 occurs for a stress state, it means that any increase in stress will result in fracture.

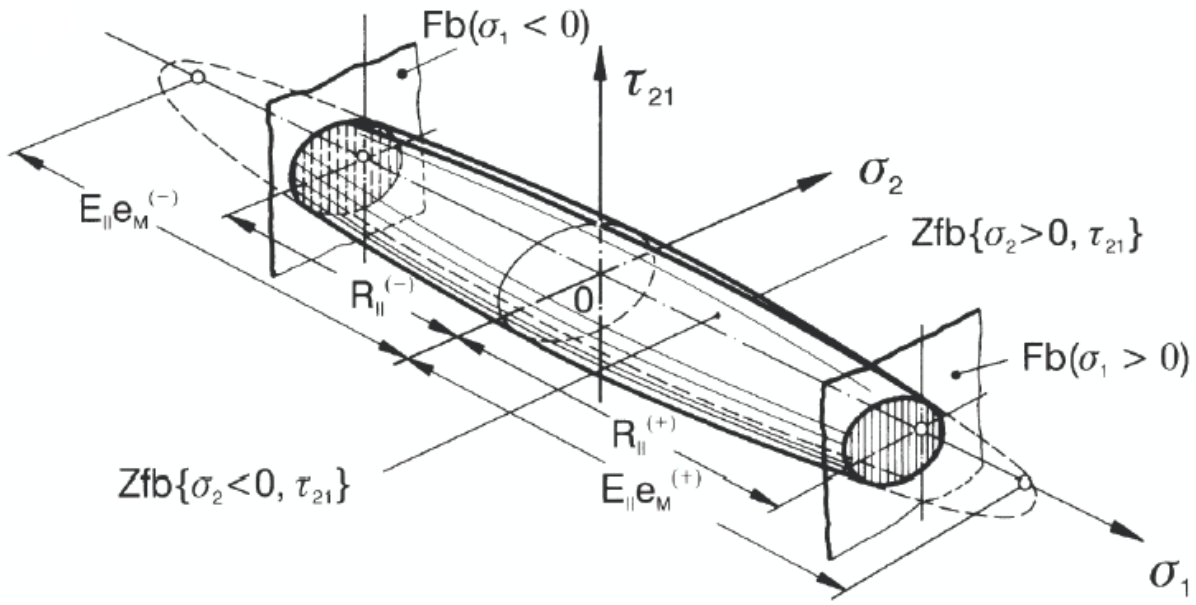

Figure 2-2 Puck's fracture cigar, [Lit.1.], p. 46

2.2.Fibre fracture conditions

As was said earlier in this chapter, fibre fracture mostly leads to lose of load-carrying capacity. In the case of FF from equation [2.1] the following fracture condition arises:

$$\mathrm{F} = \frac{\sigma_1}{R_{\parallel}^{t}} = 1 \text{ for tension} \qquad [2.2]$$

and

$$\mathrm{F} = \frac{\sigma_1}{-R_{\parallel}^{c}} = 1 \text{ for compression} \qquad [2.3]$$

For both equations we have to remember to put values as positive values. If F<1, it means that fracture limit has not been exceeded.

More precise calculations show that actually the composite stress σ_1 matters, but rather fibre direction stress σ_{1f}. The stress in fibre does not depend only on parallel stresses, but on transverse stresses. This happens due to Poisson's ratio influence. However, fracture conditions obtained with equations [2.2],[2.3] differ by only a few percent in comparison with [σ_1,σ_2,τ_{21}] stress combinations, in which σ_2 was taken into account. Moreover, experimental researches demonstrated that shear buckling of the fibres elastically embedded in the matrix is what is involved in the case of fibre fracture under a compressive stress σ_1.

2.3. Inter-fibre fracture

Inter-fibre fracture is caused by stress σ_2,σ_3,τ_{23},τ_{31},τ_{21}. It happens since matrix and fibre/matrix-interface are affected directly by these stresses which act on planes parallel to the fibres.

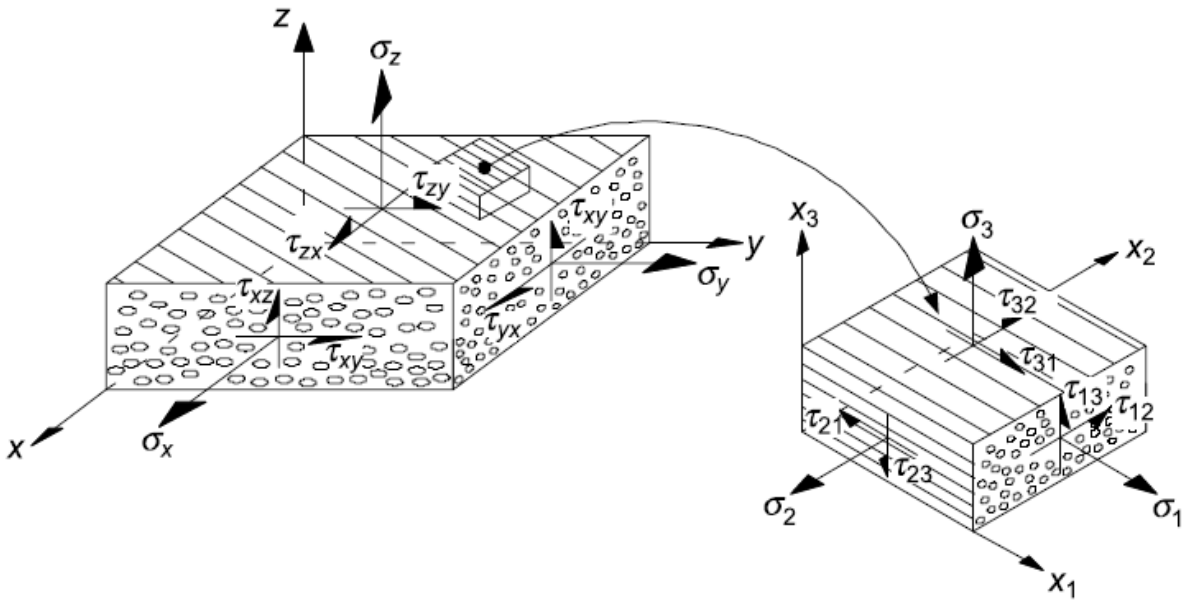

Figure 2-3 Three dimensional stressing in local COS and laminate COS, [Lit.2.], p. 12.

As we see in Fig. 2-3, we single out two different coordinate system and two expressions of stress vector as well:

$$\{\sigma\} = (\sigma_1, \sigma_2, \sigma_3, \tau_{23}, \tau_{31}, \tau_{21})^{\mathrm{T}} \; - \text{fibre coordinate system}$$

$$\{\sigma'\} = \left(\sigma_x, \sigma_y, \sigma_z, \tau_{yz}, \tau_{xz}, \tau_{xy}\right)^{\mathrm{T}} - \text{ laminate or compoment COS}$$

2.3.1. Action planes and fracture planes

The fracture limit of a material is determined by the stresses on the fracture plane. Following the plane fracture criteria of Puck, is it very important what is the kind of fracture and what is the action plane where the fracture occurs. Combined stresses acting on a common action plane have to be related to strengths of that specific action plane (cp. Fig. [2-4]). These strengths are the combination of a single stress $\sigma_{\perp}$ or $\tau_{\perp\parallel}$ or $\tau_{\perp\perp}$ that the action plane can carry. In the need of distinguish fraction resistance of the action plane and strengths, there has been introduced the term fracture resistance of the action plane R^A to which the following definition has been formulated:

A fracture resistance of the action plane is the resistance (expressed in the dimension of a stress) by which an action plane resists its own fracture due to a stress in the considered action plane caused by one of the basic stressing $\sigma_{\perp}$ or $\tau_{\perp\parallel}$ or $\tau_{\perp\perp}$. ([Lit.1.],p. 48.]

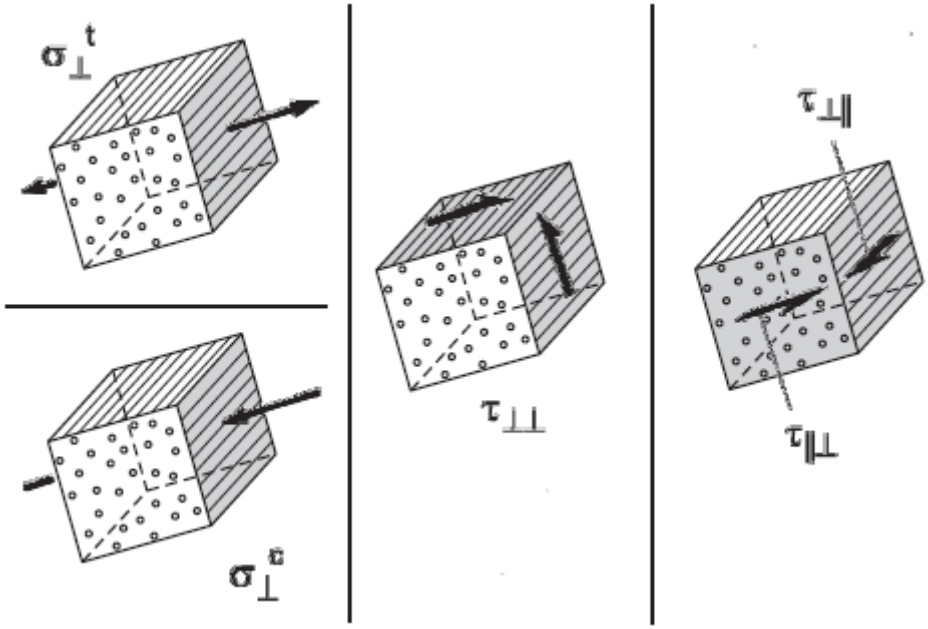

Figure 2-4 Basic stressings and their action planes, [Lit.1.], Page 48.

In need to determine the common strength of a material, it is enough to divide the maximum bearable load by the cross section area. It is significant to specify whether the fracture has occurred in the action plane of the applied stresses or not. In Fig.2-5 it is shown that not always it happens.

As we can see in almost all cases a tensile stress $\sigma_{\perp}^{t}$ leads to a fracture plane perpendicular to the applied stress. In this case the fracture plane and the action plane of the applied stress correspond to each other. Hence to this fact, the strength of the material $R_{\perp}^{t}$ (material resistance for transversal tension stress) and the fracture resistance of the action plane $R_{\perp}^{A\,t}$ will have the same value. Same case is with measuring $R_{\perp\parallel}^{A}$. It will have the same value as $R_{\perp\parallel}$.

Contrary to the two cases above, a single compressive stressing based on $\sigma_{\perp}^{c}$ cannot separate the material in its action plane which is perpendicular to stress $\sigma_{\perp}^{c}$. The element fractures due to the resulting shear stressing $\tau_{\perp\perp}$ on an oblique fracture plane. What is more it is impossible to achieve a fracture in the action plane of an applied $\tau_{\perp\perp}$, the element fractures due to a tensile stressing $\sigma_{\perp}^{t}$ on an oblique fracture plane.

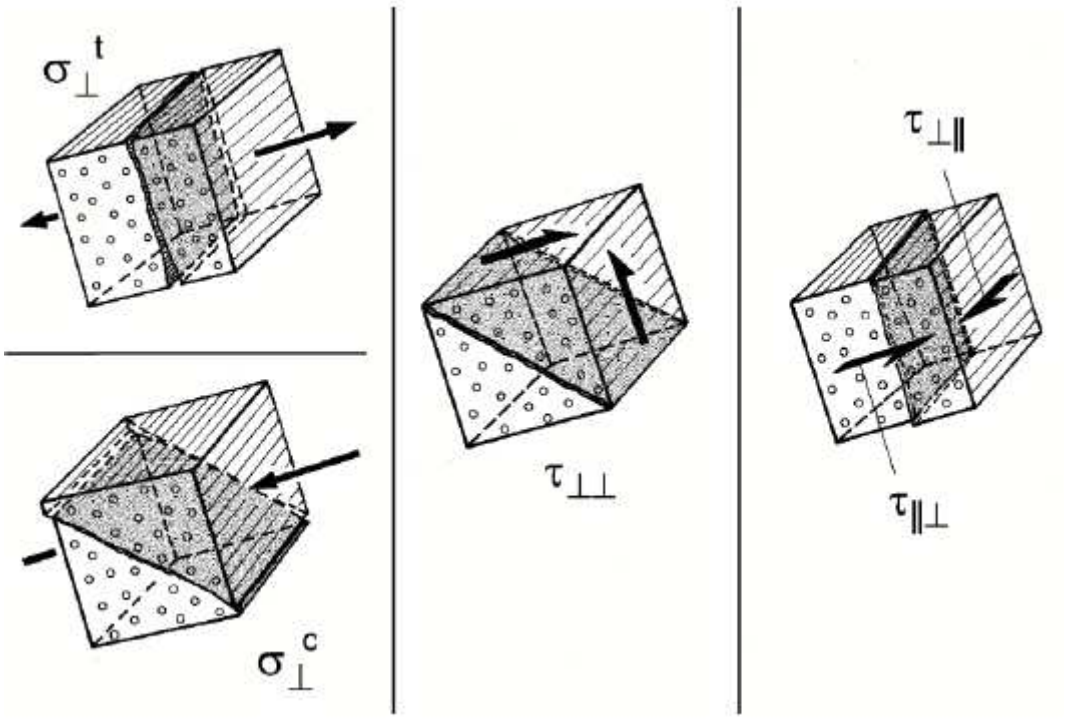

Figure 2-5 Fracture planes, [Lit.1.], Page 49

From these considerations we can achieve a conclusion that there are only three stresses that can act on a common action plane: $\sigma_\perp, \tau_{\perp\parallel}$ and $\tau_{\perp\perp}$. It means that there is a need of three fracture resistances of the action plane R_A. Two of them can be provided from usual strengths of material. The last one $R^A_{\perp\perp}$ must be calculated in another way.

2.3.2. Fracture modes

The consequence of using plane-related fracture hypothesis, is that there is an infinite number of action planes that are potential fracture planes. Therefore, before fracture stresses can be calculated, the action plane with the highest risk of fracture has to be found. It requires a numerical search.

To find this proper plane the stretch factor f_s must be calculated for a number of sections between $\theta = [-90°, 90°]$, normally with the iteration step equal to 1°. The term f_s is the factor, by which these plane stress vector $\vec{\sigma} = [\sigma_n(\theta), \tau_{nt}(\theta), \tau_{n1}(\theta)]$ on the considered action plane must be increased to cause the fracture. The normal stress $\sigma_n^{t,c}$is the stress acting perpendicularly to action plane (*c* for compression, *t* for tension and index *n* means that the direction of stress is perpendicular to action plane). Shear stresses τ_{nt}, τ_{n1} are the stresses acting on action plane: shear stresses τ_{nt} are the stresses perpendicular to fibre direction and shear stresses τ_{n1} are the stresses parallel to fibre direction, (cp. Fig. 2-6). The

index *t* means that stresses are perpendicular to fibre direction and *1* that they are parallel to fibre direction.

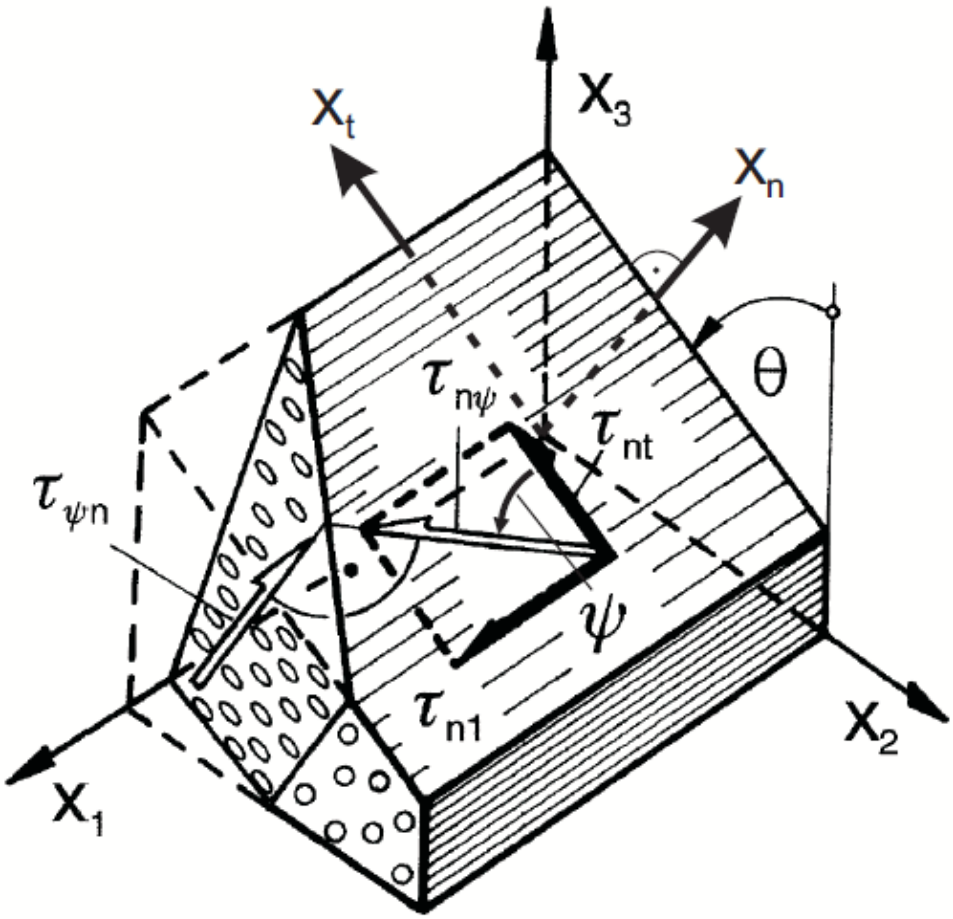

Figure 2-6 Shear stresses on action plane, [Lit.1.], Page 50

In order to a better interpretation and explanation of action planes and states of stress the nomenclature of stresses will be change now into representation of fibre coordinate system $\{\sigma\} = (\sigma_1, \sigma_2, \sigma_3, \tau_{23}, \tau_{31}, \tau_{21})^{\mathrm{T}}$.

Based on the state of stress and defined action plane we can determine three modes. Modes describe what kind of fracture occurs. Therefore we can achieve mode A, B and C. The first one, mode A, is the case when action plane is parallel to fibre direction and fracture is caused by normal tension stresses perpendicular to fibre direction σ_2^t with or without accompaniment of shear stresses τ_{21} or only by shear stresses τ_{21}. Therefore, in the action plane we can achieve three different states of stresses: $\vec{\sigma} = [\sigma_n > 0, \tau_{nt} = 0, \tau_{n1} = 0]$, $\vec{\sigma} = [\sigma_n > 0, \tau_{nt} = 0, \tau_{n1} \neq 0]$ and $\vec{\sigma} = [\sigma_n = 0, \tau_{nt} = 0, \tau_{n1} \neq 0]$. Mode B will be achieved, when normal compressive stresses σ_2^c occurs with accompaniment of shear stresses τ_{21} and the action plane will be perpendicular to normal stresses. It this case the stress vector on action plane has the following representation: $\vec{\sigma} = [\sigma_n < 0, \tau_{nt} = 0, \tau_{n1} \neq 0]$. Mode C is the

mode when action plane occurs when the angle between plane perpendicular to normal stresses and the action plane is different from 0°. In this case, stressing causes transversal shear stresses in action plane τ_{nt}. Therefore, we can achieve two different state of stress in the action plane: $\vec{\sigma} = [\sigma_n < 0, \tau_{nt} \neq 0, \tau_{n1} \neq 0]$ and $\vec{\sigma} = [\sigma_n < 0, \tau_{nt} \neq 0, \tau_{n1} = 0]$.

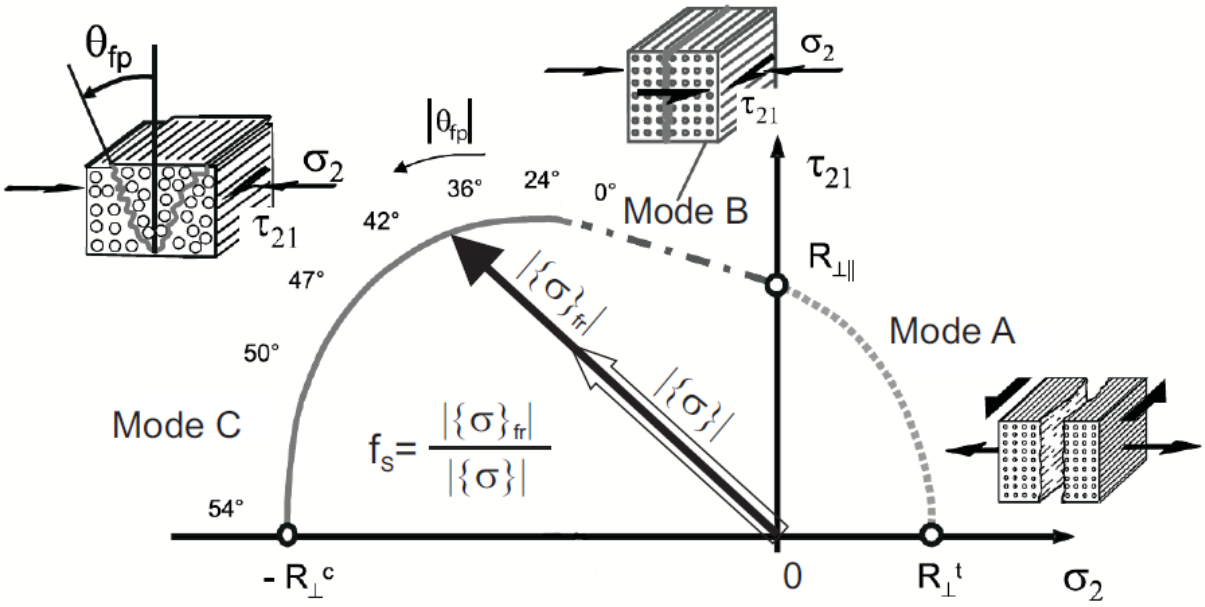

Figure 2-7 Vizualization of stress factor, [Lit.1.], Page 51

$$f_E = \frac{1}{f_s} = \frac{lenght\ of\ actual\ stress\ vector\ \vec{\sigma}}{length\ of\ the\ vector\ \overrightarrow{\sigma_{fr}}\ of\ the\ stresses\ leading\ to\ fracture} \qquad [2.4]$$

The factor f_E is the stress exposure and this is the direct measure for the risk of fracture. For each mode (cp. Fig. 2-7) it should be calculated with different equations and for three-dimensional stresses proper ones are shown below.

For mode A ($\sigma_2 \geq 0$):

$$f_E|_{\theta_{fp}=0°} = \frac{1}{R_{\perp\parallel}}\left[\sqrt{\left(\frac{R_{\perp\parallel}}{R_{\perp}^{t}} - p_{\perp\parallel}^{t}\right)^2 \sigma_2^2 + \tau_{21}^2} + p_{\perp\parallel}^{t}\sigma_2\right] = 1 \qquad [2.5]$$

For mode B:

$$f_E|_{\theta_{fp}=0°} = \frac{1}{R_{\perp\parallel}}\left[\sqrt{\tau_{21}^2 + \left(p_{\perp\parallel}^{c}\sigma_2\right)^2} + p_{\perp\parallel}^{c}\sigma_2\right] = 1 \qquad [2.6]$$

For mode C:

$$f_E|_{\theta_{fp}\ equ\ (8)} = \frac{\tau_{21}^2}{4\left(R_{\perp\parallel} + p_{\perp\parallel}^c R_{\perp\perp}^A\right)^2} * \frac{(-R_\perp^c)}{\sigma_2} + \frac{\sigma_2}{(-R_\perp^c)} = 1 \qquad [2.7]$$

$$cos\theta_{fp} = \sqrt{\frac{1}{2(1+p_{\perp\perp}^c)}\left[\left(\frac{R_{\perp\perp}^A}{R_{\perp\parallel}}\right)^2 * \left(\frac{\tau_{21}}{\sigma_2}\right)^2 + 1\right]} \qquad [2.8]$$

The meaning of "p" parameters will be explained later on.

2.3.3. Action plane stresses

As written above, in this criteria the stress vector is formulated with three stresses $\vec{\sigma} = [\sigma_n(\theta), \tau_{nt}(\theta), \tau_{n1}(\theta)]$, which act on parallel-to-fibre section planes. The applied stresses which have to be transmitted by the matrix and the fibre/matrix interfaces are of main importance for an inter-fibre fracture. The action plane related stresses are derived from the applied stresses as shown in below equations:

$$\sigma_n(\theta) = \sigma_2 * cos^2\theta + \sigma_3 * sin^2\theta + 2 * \tau_{23} * sin\theta * cos\theta \qquad [2.9]$$

$$\tau_{nt}(\theta) = -\sigma_2 * sin\theta * cos\theta + \sigma_3 * sin\theta * cos\theta + \tau_{23} * (cos^2\theta - sin^2\theta) \qquad [2.10]$$

$$\tau_{n1}(\theta) = \tau_{31} * sin\theta + \tau_{21} * cos\theta \qquad [2.11]$$

For numerical calculations it is more comfortable to write it matrix notification:

$$\begin{bmatrix}\sigma_n(\theta)\\ \tau_{nt}(\theta)\\ \tau_{n1}(\theta)\end{bmatrix} = \begin{bmatrix} c^2 & s^2 & 2sc & 0 & 0\\ -sc & sc & (c^2 - s^2) & 0 & 0\\ 0 & 0 & 0 & s & c\end{bmatrix}\begin{bmatrix}\sigma_2\\ \sigma_3\\ \tau_{23}\\ \tau_{31}\\ \tau_{21}\end{bmatrix} \qquad [2.12]$$

where $c = cos\theta$ and $s = sin\theta$

As we can see, IFF is mainly caused by the stresses $\sigma_2, \sigma_3, \tau_{23}, \tau_{31}, \tau_{21}$. The action plane of the stress σ_1 is perpendicular to any IFF action plane. Therefore the stress vector $\vec{\sigma} = [\sigma_n(\theta), \tau_{nt}(\theta), \tau_{n1}(\theta)]$ does not depend on this stress. However, the stress σ_1 has some influence on IFF and it is weakening the material. This phenomenon will be described more precisely in section 2.5 of this thesis.

When the normal stress σ_n is a positive stress (tensile), it assists the shear stresses τ_{nt} and τ_{n1} in causing IFF. In opposite, a compressive normal stress will slow down the IFF. Due to this fact, two sets of equations should be taken into account, depending on normal stress sign.

With the new equations and stresses now it is possible to make statements regarding the direction of fracture plane (cp. Fig. 2-7). In the figure 2-8 a) we can again see the action plane stresses $\sigma_n, \tau_{nt}, \tau_{n1}$ and the shear vector $\tau_{n\psi}$ (shear stresses τ_{nt}, τ_{n1} are components of this vector). Sub-figure b) shows us the master fracture body based on equations [2.13]-[2.18]. The other four sub-figures shows cross-section of the master fracture body. Sub-figure c) determine the cross-section for $\sigma_n = 0$. Sub-figure d) is the cross-section for $\tau_{nt} = 0$ and f) for $\tau_{n1} = 0$. The sub-figure e) is the cross-section of constant ψ angle, the angle between stresses τ_{n1} and τ_{nt}. As we can see, aster fracture body is defined by its cross sections.

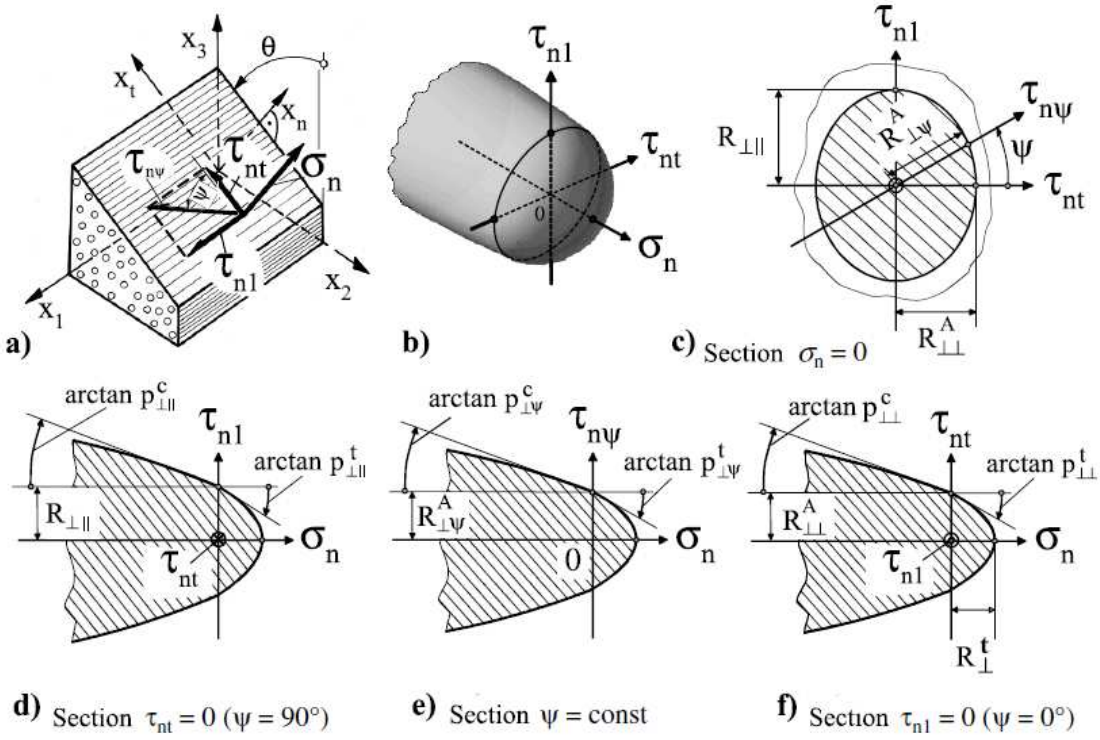

Figure 2-8 Action plane stresses, [Lit.2.], Page 44

The intersection stress exposure $f_E(\theta)$, dependent on angle and type of normal stress, is calculated with the following equations.

For $\sigma_n \geq 0$:

$$f_E(\theta) = \sqrt{\left[\left(\frac{1}{R_\perp^t} - \frac{p_{\perp\psi}^t}{R_{\perp\psi}^A}\right)\sigma_n\right]^2 + \left(\frac{\tau_{nt}}{R_{\perp\perp}^A}\right)^2 + \left(\frac{\tau_{n1}}{R_{\perp\parallel}}\right)^2} + \frac{p_{\perp\psi}^t}{R_{\perp\psi}^A}\sigma_n \qquad [2.13]$$

For $\sigma_n < 0$:

$$f_E(\theta) = \sqrt{\left(\frac{\tau_{nt}}{R^A_{\perp\perp}}\right)^2 + \left(\frac{\tau_{n1}}{R^A_{\perp\parallel}}\right)^2 + \left(\frac{p^c_{\perp\psi}}{R^A_{\perp\psi}}\sigma_n\right)^2} + \frac{p^c_{\perp\psi}}{R^A_{\perp\psi}}\sigma_n \qquad [2.14]$$

where appropriate factors depended on ψ angle are calculated as follows:

$$\frac{p^t_{\perp\psi}}{R^A_{\perp\psi}} = \frac{p^t_{\perp\perp}}{R^A_{\perp\perp}}cos^2\psi + \frac{p^t_{\perp\parallel}}{R_{\perp\parallel}}sin^2\psi \qquad [2.15]$$

$$\frac{p^c_{\perp\psi}}{R^A_{\perp\psi}} = \frac{p^c_{\perp\perp}}{R^A_{\perp\perp}}cos^2\psi + \frac{p^c_{\perp\parallel}}{R_{\perp\parallel}}sin^2\psi \qquad [2.16]$$

$$cos^2\psi = 1 - sin^2\psi = \frac{\tau^2_{nt}}{\tau^2_{nt} - \tau^2_{n1}} \qquad [2.17]$$

$$[f_{E\,IFF}(\theta)]_{max} = f_{E\,IFF(\theta_{fp})} \qquad [2.18]$$

where the used symbol θ_{fp} is the angle of fracture plane.

Now also we can calculate missing factor $R^A_{\perp\perp}$:

$$R^A_{\perp\perp} = \frac{R^c_{\perp}}{2(1 + p^c_{\perp\perp})} \qquad [2.19]$$

Parameters used in above equations $p^c_{\perp\parallel}, p^t_{\perp\parallel}, p^t_{\perp\perp}, p^c_{\perp\perp}$ are so called slope parameters. These values should be determined on the experimental way. But if there is no experimental data available, there are recommended values, which should be used (cp. Table.[2-1]).

	$p^c_{\perp\parallel}$	$p^t_{\perp\parallel}$	$p^c_{\perp\perp} = p^t_{\perp\perp}$
GFRP	0.25	0.30	0.20 to 0.25
CFRP	0.30	0.35	0.25 to 0.30

Table 2-1 Slope parameters, [Lit.1.], p. 57

These are values for glass-fibre-reinforced (GFRP) plastics and carbon-fibre-reinforced plastics (CFRP).

Assuming above considerations we can distinguish three modes according to Table [2-2].

Mode A $\theta_{fp} = 0°$	Mode B $\theta_{fp} = 0°$	Mode C $\theta_{fp} \neq 0°$
$\{\sigma_n^t \quad 0 \quad 0\}$ $\{\sigma_n^t \quad 0 \quad \tau_{n1}\}$ $\{0 \quad 0 \quad \tau_{n1}\}$	$\{\sigma_n^c \quad 0 \quad \tau_{n1}\}$	$\{\sigma_n^c \quad \tau_{nt} \quad \tau_{n1}\}$ $\{\sigma_n^c \quad \tau_{nt} \quad 0\}$

Table 2-2 Different modes and their stresses, [Lit.1.], p. 59

2.4. Material law

Now when we know how Puck's criteria works, we can skip to material degradation factors, but first some words about material law must be said.

Unidirectional fibre-reinforced lamina must be described with strength parameters, these are $R_{\parallel}^t, R_{\parallel}^c, R_{\perp}^t, R_{\perp}^c, R_{\perp\perp}, R_{\perp\parallel}, R_{\perp\perp}^A$, as well as material constants. This means Young and shear modulus, and Poisson's ratio: $E_{\parallel}, E_{\perp}, G_{\perp\parallel}, \upsilon_{\perp\parallel}, \upsilon_{\parallel\perp}, \upsilon_{\perp\perp}$. With the material constants we can build material stiffness matrix (elasticity matrix). Basing on this matrix and defined state of strain, we can determine the state of stress, see equation 2.20.

$$[\sigma_1, \sigma_2, \sigma_3, \tau_{23}, \tau_{31}, \tau_{21}]^T = [E] * [\sigma_1, \sigma_2, \sigma_3, \gamma_{12}, \gamma_{13}, \gamma_{23}]^T \qquad [2.20]$$

Where [E] is the stiffness matrix.

For Puck's criteria we are interested in calculating stresses that occurs under applied load or displacement. Let us precise above equation (19)(cp. [Lit.1.], p. 21.]).

$$\begin{bmatrix} \sigma_1 \\ \sigma_2 \\ \sigma_3 \\ \tau_{12} \\ \tau_{13} \\ \tau_{23} \end{bmatrix} = \begin{bmatrix} D_{1111} & D_{1122} & D_{1133} & 0 & 0 & 0 \\ D_{2211} & D_{2222} & D_{2233} & 0 & 0 & 0 \\ D_{3311} & D_{3322} & D_{3333} & 0 & 0 & 0 \\ 0 & 0 & 0 & D_{1212} & 0 & 0 \\ 0 & 0 & 0 & 0 & D_{1313} & 0 \\ 0 & 0 & 0 & 0 & 0 & D_{2323} \end{bmatrix} * \begin{bmatrix} \varepsilon_1 \\ \varepsilon_2 \\ \varepsilon_3 \\ \gamma_{12} \\ \gamma_{13} \\ \gamma_{23} \end{bmatrix} \qquad [2.21]$$

The components of the elasticity matrix are given below:

$$D_{1111} = E_1(1 - \upsilon_{23}\upsilon_{32})\Upsilon \qquad [2.22]$$

$$D_{2222} = E_2(1 - \upsilon_{13}\upsilon_{31})\Upsilon \qquad [2.23]$$

$$D_{3333} = E_3(1 - \upsilon_{12}\upsilon_{21})\Upsilon \qquad [2.24]$$

$$D_{1122} = D_{2211} = E_1(\upsilon_{21} + \upsilon_{31}\upsilon_{23})\Upsilon = E_2(\upsilon_{12} + \upsilon_{32}\upsilon_{13})\Upsilon \qquad [2.25]$$

$$D_{1133} = D_{3311} = E_1(\upsilon_{31} + \upsilon_{21}\upsilon_{32})\Upsilon = E_3(\upsilon_{13} + \upsilon_{12}\upsilon_{23})\Upsilon \qquad [2.26]$$

$$D_{2233} = D_{3322} = E_2(\upsilon_{32} + \upsilon_{12}\upsilon_{31})\Upsilon = E_3(\upsilon_{23} + \upsilon_{21}\upsilon_{13})\Upsilon \qquad [2.27]$$

$$D_{1212} = G_{12} \qquad [2.28]$$

$$D_{1313} = G_{13} \qquad [2.29]$$

$$D_{2323} = G_{23} \qquad [2.30]$$

where Υ factor is calculate as follows:

$$\Upsilon = \frac{1}{1 - \upsilon_{12}\upsilon_{21} - \upsilon_{23}\upsilon_{32} - \upsilon_{13}\upsilon_{31} - 2\upsilon_{21}\upsilon_{32}\upsilon_{13}} \qquad [2.31]$$

There are also some stability restriction on the engineering constants:

$$E_1, E_2, E_3, G_{12}, G_{13}, G_{23} > 0 \qquad [2.32]$$

$$|\upsilon_{12}| < \left(\frac{E_1}{E_2}\right)^{\frac{1}{2}} \; or \; |\upsilon_{21}| < \left(\frac{E_2}{E_1}\right)^{\frac{1}{2}} \qquad [2.33]$$

$$|\upsilon_{13}| < \left(\frac{E_1}{E_3}\right)^{\frac{1}{2}} \; or \; |\upsilon_{31}| < \left(\frac{E_3}{E_1}\right)^{\frac{1}{2}} \qquad [2.34]$$

$$|\upsilon_{23}| < \left(\frac{E_2}{E_3}\right)^{\frac{1}{2}} \; or \; |\upsilon_{32}| < \left(\frac{E_3}{E_2}\right)^{\frac{1}{2}} \qquad [2.35]$$

$$1 - \upsilon_{12}\upsilon_{21} - \upsilon_{23}\upsilon_{32} - \upsilon_{13}\upsilon_{31} - 2\upsilon_{21}\upsilon_{32}\upsilon_{13} > 0 \qquad [2.36]$$

The equations shown above lead to calculate the stress vector which must be multiplied by rotation matrix to achieve 3-element stress vector $\vec{\sigma} = [\sigma_n(\theta), \tau_{nt}(\theta), \tau_{n1}(\theta)]$ (see section 2.3.3) for Puck's criteria usage.

2.5.Weakening factor

As was said before, the stress σ_1 does not have any influence on the inter-fibre fracture. It is due to the fact that the action plane of σ_1 is perpendicular to the action plane of the stresses $\sigma_n, \tau_{nt}, \tau_{n1}$. Nevertheless, some effects make us to take σ_1 under consideration, while calculating IFF. For instance, when fibre fracture marks the fracture of a large number of elementary fibres, it causes the decrease of lamina's load-bearing capacity in the direction of fibre direction over a macro-region. What is more, in the event of tensile stress σ_1, some fibres can break even before the FF limit of lamina has been reached. Also, in the case of compressive stress, it is possible that individual bundles of fibres could already start kinking before the total fracture occurs. These micro fibre fractures cause local damage in the lamina which takes the form of micro fractures in the matrix material. It weakens the fibre matrix cohesion and hence reduce its resistance to IFF. It is called weakening effect.

The way to include in IFF analysis the weakening effect, appropriate to the physical circumstances, is to multiply the action-plane-fracture resistances by a degradation factor η_{w1}, when "w" in index means weakening and "1" that is due to the fact of σ_1 influence. For simplification of equations and calculations it is assumed that the weakening factor has the same value for all three action-plane-resistances $R_{\perp}^{t}, R_{\perp\perp}^{A}, R_{\perp\parallel}$. This assumption has the effect that the inclination of the fracture given by the fracture plane angle θ_{fp} and the IFF mode connected with it are not affected by the weakening which is now dependent on σ_1, because σ_1 does not depend on θ.

It is obvious that the reduction of fracture resistances results in an increased stress exposure. Therefore the stress exposure f_{E1} when taking into account the influence of σ_1 becomes:

$$f_{E1} = \frac{f_{E0}}{\eta_{w1}} \qquad [2.37]$$

The only work now is to find the weakening factor. It is derived by the following equations (see Lit.1. Page 46., eq. (4.26)):

$$\eta_{w1} = \frac{c\left(a\sqrt{c^2(a^2 - s^2) + 1} + s\right)}{(ca)^2 + 1} \qquad [2.38]$$

Where:

$$c = \frac{f_{E0}}{f_{E(FF)}} \text{ and } a = \frac{1 - s}{\sqrt{1 - m^2}} \qquad [2.39]$$

The range of validity of the weakening factor is gives by:

$$\frac{1}{s} \geq \frac{f_{E0}}{f_{E(FF)}} \geq m \qquad [2.40]$$

As far as there are no reliable experimentally determined values for parameters s and m, some values must be chosen. It is recommended to use value s=m=0.5 (cp. [Lit.1.], p. 62.).

2.6. Material degradation

The purpose of using Puck's criteria, is not only to determine when the fracture in lamina occurs, but also how the material will behave after this happened. The stress exposure $f_E = 1$ denotes the state of stress in a lamina where the first macroscopic crack through the entire thickness of the respective lamina occurs. In the case of a composite

structure, reaching a single lamina's fracture condition is not equivalent with the disintegration of the whole material. In a such confined lamina a further increased applied load starts a successive damage evolution process in the form of a growing macroscopic crack density. This means the reduction of the lamina's load-bearing capacity and this process is called degradation.

The degradation process of a lamina due to an increasing macroscopic crack density is represented by the reduction of the stiffness. This means that under the same load applied to the structure, there will be a change of displacement.

$$\text{reduced stiffness} = \eta * \text{original stiffness}$$

Loading a laminate in-plane, the lamina is only exposed to transverse stress σ_2 and in-plane shear stress τ_{12}. It is causing that only transverse Young's modulus E_2 and the in-plane shear modulus G_{12} are about to be degraded. After several experiments (cp. Lit. 6), it was suggested that Poisson's ratio should stay constant.

$$E_2^{red} = \begin{cases} \eta * E_2^{orig} \text{ for tensile } \sigma_n \text{ on the fracture plane} \\ E_2^{orig} \text{ for compresive } \sigma_n \text{ on the fracture plane} \end{cases} \qquad [2.41]$$

$$G_{12}^{red} = \eta * G_{12}^{orig} \qquad [2.42]$$

The reduction factor is calculated as follows:

$$\eta(f_{E\,IFF}) = \frac{1-\eta_R}{1+a(f_{E\,IFF}-1)^{\zeta}} + \eta_R \text{ for } f_{E\,IFF} > 1 \qquad [2.43]$$

As we can see the exposure value $f_E = 1$ results in reduction factor value $\eta = 1$.

Factors a and ζ used in equation [2.43] must be chosen in base of experimnets. Several experiments showed that reasonable values are $a = [0.95; 5.5]$ and $\zeta = [1.17; 1.5]$ (see Lit.1., Page 80.) depending on the material. It was also suggested to reduce shear modulus less than Young's modulus. It is made by using different residual stiffness fractions η_R for these modulus. There is a different value for residual stiffness fraction for Young's modulus η_{RE} and for residual stiffness fraction for shear modulus η_{RG}. These values also must be defined experimentaly and differently for each material. Therefore we will achieve two different equations for Young's modulus degradation and shear modulus:

$$\eta_E(f_{E\,IFF}) = \frac{1-\eta_{RE}}{1+a(f_{E\,IFF}-1)^{\zeta}} + \eta_{RE} \text{ for } f_{E\,IFF} > 1 \qquad [2.44]$$

$$\eta_G(f_{E\,IFF}) = \frac{1-\eta_{RG}}{1+a(f_{E\,IFF}-1)^{\zeta}} + \eta_{RG} \text{ for } f_{E\,IFF} > 1 \qquad [2.45]$$

And equations [2.41] and [2.42] will now look as follows:

$$E_2^{red} = \begin{cases} \eta_E * E_2^{orig} \text{ for tensile } \sigma_n \text{ on the fracture plane} \\ E_2^{orig} \text{ for compresive } \sigma_n \text{ on the fracture plane} \end{cases} \qquad [2.46]$$

$$G_{12}^{red} = \eta_G * G_{12}^{orig} \qquad [2.47]$$

3. Degradation procedure

The main reason for using Puck's criteria is to provide degradation process of composite structure with Abaqus software. For this purpose an user-defined material behavior subroutine (UMAT) is written in Fortran code and then implemented to Abaqus Finite Element numerical calculations. It is written for implicit method and will include all presented above part's of Puck's theory for the fibre fracture and inter-fibre fracture prediction of the degradation rule.

Abaqus by itself has many calculation options in its software, also for composites structure. Nevertheless it allows to model only a 2-dimensional model and does not have Puck's criteria definition in its library. Therefore there is a need to use a user subroutine that allows us to define material law for every integration point in the model and change material constants due to degradation process for every integration point. The only suitable subroutine for this job is the user-defined material behavior subroutine called UMAT (cp. [Lit.4.]). Between this subroutine and Abaqus software we can achieve two-way communication and thanks to that obtain necessary values from Abaqus main program, update them in UMAT subroutine and send them back. This communication occurs every increment in every step during analysis. To describe more precisely the whole process of this communication, the heading of this subroutine is needed to be introduced first (see also Appendix 1.):

```
      SUBROUTINE UMAT(STRESS,STATEV,DDSDDE,SSE,SPD,SCD,
     1 RPL,DDSDDT,DRPLDE,DRPLDT,
     2 STRAN,DSTRAN,TIME,DTIME,TEMP,DTEMP,PREDEF,DPRED,CMNAME,
     3 NDI,NSHR,NTENS,NSTATV,PROPS,NPROPS,COORDS,DROT,PNEWDT,
     4 CELENT,DFGRD0,DFGRD1,NOEL,NPT,LAYER,KSPT,KSTEP,KINC)
C
      INCLUDE 'ABA_PARAM.INC'
C
      CHARACTER*80 CMNAME
      DIMENSION STRESS(NTENS),STATEV(NSTATV),
     1 DDSDDE(NTENS,NTENS),DDSDDT(NTENS),DRPLDE(NTENS),
     2 STRAN(NTENS),DSTRAN(NTENS),TIME(2),PREDEF(1),DPRED(1),
     3 PROPS(NPROPS),COORDS(3),DROT(3,3),DFGRD0(3,3),DFGRD1(3,3)
```

This is the heading that has to be included in every UMAT subroutine and it described what information will be provided by Abaqus the main program to the subroutine and what information should be send back to Abaqus by the subroutine. The first group of variable, mentioned after the name of the subroutine, are the information gained from Abaqus. The second group are information send back to Abaqus after every increment in every step.

The definition of variables used in UMAT subroutine in according to [Lit.4.]l:

STRESS(NTENS)- this array is passed in as the stress tensor at the beginning of the increment and must be updated in this routine to be the stress tensor at the end of the increment. It contains the stresses $\sigma_1, \sigma_2, \sigma_3, \tau_{12}, \tau_{13}, \tau_{23}$.

STATEV(NSTATV)- an array containing the solution-dependent state variables. These are passed in as the values at the beginning of the increment. In all cases STATEV must be returned as the values at the end of the increment. In other words, these are the values that we want to update after every increment. It is very important variable in the context of communication with Abaqus. With this variables we are allowed to change lamina's elasticity matrix due to degradation process. The exect entries are stresses, residual stiffness fraction for Young's modulus and shear modulus, and IFF. In the Fig. 3-1 it is shown how solution-dependent state variables are activated in Abaqus.

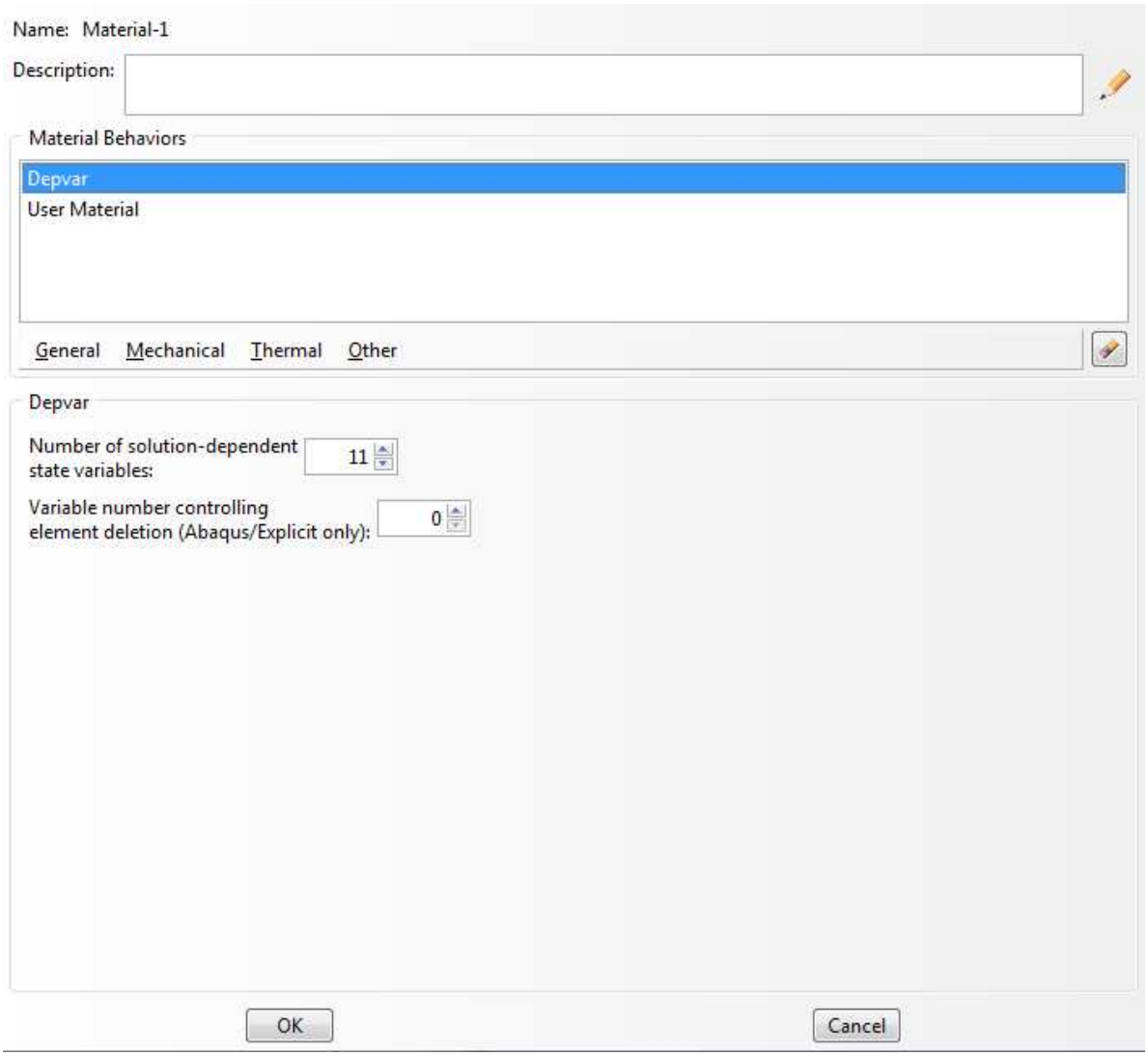

Figure 3-1 Solution depended variables settings

`DDSDDE(NTENS,NTENS)-` Jacobian matrix of the constitutive model, $\frac{\Delta\sigma}{\Delta\varepsilon}$, where $\Delta\sigma$ are the stress increments and $\Delta\varepsilon$ are the strain increments (cp. equation 3-47). DDSDDE(I,J) defines the change in the n-th stress component at the end of the UMAT. In linear problems it is equal to elasticity matrix (also called secant stiffness matrix).

$$J = \frac{\Delta\sigma}{\Delta\varepsilon}\begin{bmatrix} \frac{\Delta\sigma_1}{\Delta\varepsilon_1} & \frac{\Delta\sigma_1}{\Delta\varepsilon_2} & \frac{\Delta\sigma_1}{\Delta\varepsilon_3} & \frac{\Delta\sigma_1}{\Delta\gamma_{12}} & \frac{\Delta\sigma_1}{\Delta\gamma_{13}} & \frac{\Delta\sigma_1}{\Delta\gamma_{23}} \\ \frac{\Delta\sigma_2}{\Delta\varepsilon_1} & \frac{\Delta\sigma_2}{\Delta\varepsilon_2} & \frac{\Delta\sigma_2}{\Delta\varepsilon_3} & \frac{\Delta\sigma_2}{\Delta\gamma_{12}} & \frac{\Delta\sigma_2}{\Delta\gamma_{13}} & \frac{\Delta\sigma_2}{\Delta\gamma_{23}} \\ \frac{\Delta\sigma_3}{\Delta\varepsilon_1} & \frac{\Delta\sigma_3}{\Delta\varepsilon_1} & \frac{\Delta\sigma_3}{\Delta\varepsilon_3} & \frac{\Delta\sigma_3}{\Delta\gamma_{12}} & \frac{\Delta\sigma_3}{\Delta\gamma_{13}} & \frac{\Delta\sigma_3}{\Delta\gamma_{23}} \\ \frac{\Delta\tau_{12}}{\Delta\varepsilon_1} & \frac{\Delta\tau_{12}}{\Delta\varepsilon_2} & \frac{\Delta\tau_{12}}{\Delta\varepsilon_3} & \frac{\Delta\tau_{12}}{\Delta\gamma_{12}} & \frac{\Delta\tau_{12}}{\Delta\gamma_{13}} & \frac{\Delta\tau_{12}}{\Delta\gamma_{23}} \\ \frac{\Delta\tau_{13}}{\Delta\varepsilon_1} & \frac{\Delta\tau_{13}}{\Delta\varepsilon_2} & \frac{\Delta\tau_{13}}{\Delta\varepsilon_3} & \frac{\Delta\tau_{13}}{\Delta\gamma_{12}} & \frac{\Delta\tau_{13}}{\Delta\gamma_{13}} & \frac{\Delta\tau_{13}}{\Delta\gamma_{23}} \\ \frac{\Delta\tau_{23}}{\Delta\varepsilon_1} & \frac{\Delta\tau_{23}}{\Delta\varepsilon_2} & \frac{\Delta\tau_{23}}{\Delta\varepsilon_3} & \frac{\Delta\tau_{23}}{\Delta\gamma_{12}} & \frac{\Delta\tau_{23}}{\Delta\gamma_{13}} & \frac{\Delta\tau_{23}}{\Delta\gamma_{23}} \end{bmatrix} \qquad [3.47]$$

However, in our procedure we are using stiffness matrix showed in equation [2.21].

`STRAN(NTENS)-` an array containing the total strains $(\varepsilon_1, \varepsilon_2, \varepsilon_3, \gamma_{12}, \gamma_{13}, \gamma_{23})$ at the beginning of the increment. This information is provided by Abaqus at the begining of every increment.

`DSTRAN(NTENS)-` an array of strain increments.

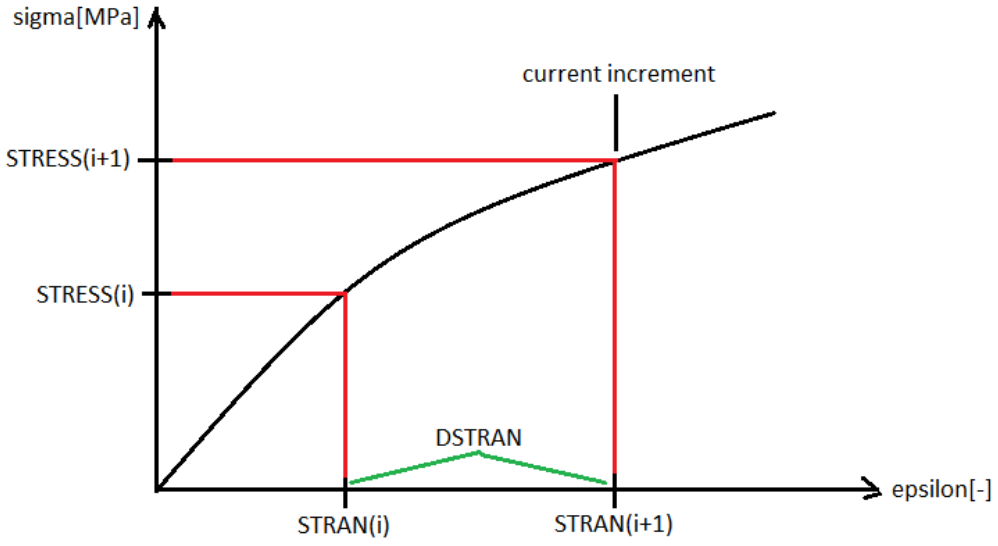

Figure 3-2 Solution process

Figure 3-1 helps us to understand what actually STRESS, STRAN and DSTRAN array contain. In the current increment point Abaqus provides state of stress from the

previous increment STRESS(i), state of total strains and the end of previous increment STRAN(i) and DSTRAN. At the end of increment, the subroutine provides information about current state of stress STRESS(i+1) and current state of total strains STRAN(i+1).

`TIME(1)-` value of the step time at the beginning of the current increment.

`TIME(2)-` value of total time at the beginning of the current increment.

`DTIME-` time increment.

Fig. 3-1 shows interpretation of TIME(1), TIME(2) and DTIME variables.

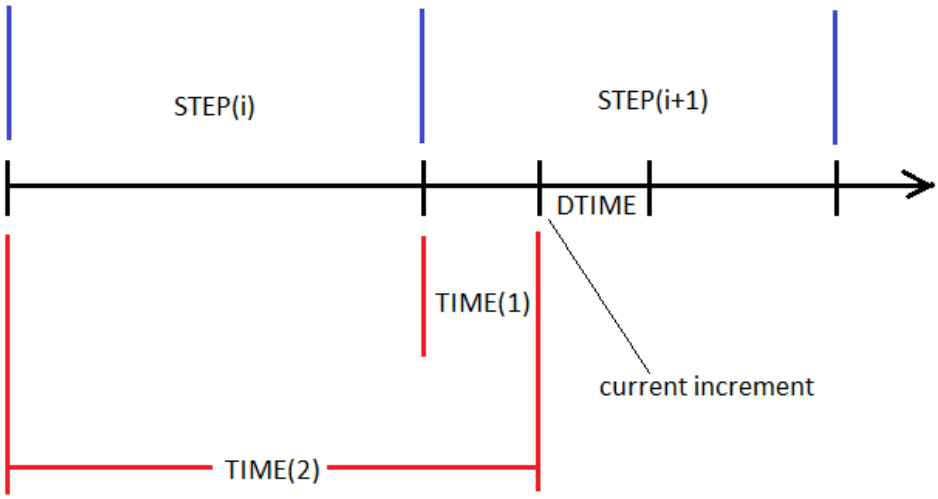

Figure 3-3 Graphical interpretation of TIME(2), TIME(1) and DTIME variables

`NDI-` number of direct stress components ($\sigma_1, \sigma_2, \sigma_3$) at this integration point

`NSHR-` number of engineering shear stress components ($\tau_{12}, \tau_{13}, \tau_{23}$) at this integration point.

`NTENS-` size of stress or strain component array (`NDI+NSHR`).

`NSTATV-` number of solution-dependent state variables that are associated with this material type. It describes how many solution-dependent variables should be sent back to the Abaqus every iteration.

`PROPS(NPROPS)-` user-specified array of material constants associated with this user material. It contains all material constants defined in the Abaqus main program.

NPROPS - user-defined number of material constants associated with this user material. It describes how many material constants will be provided by Abaqus main program.

In the Fig. 3-4 it is shown how material constants and number of these variables are set in Abaqus. In the case of laminate we can distinguish eighteen variables which are: $E_1, E_2, E_3, \upsilon_{12}, \upsilon_{13}, \upsilon_{23}, G_{12}, G_{13}, G_{23}, R_{\parallel}^{t}, R_{\parallel}^{c}, R_{\perp}^{t}, R_{\perp}^{c}, R_{\perp\parallel}, p_{\perp\parallel}^{c}, p_{\perp\parallel}^{t}, p_{\perp\perp}^{c}, p_{\perp\perp}^{t}$.

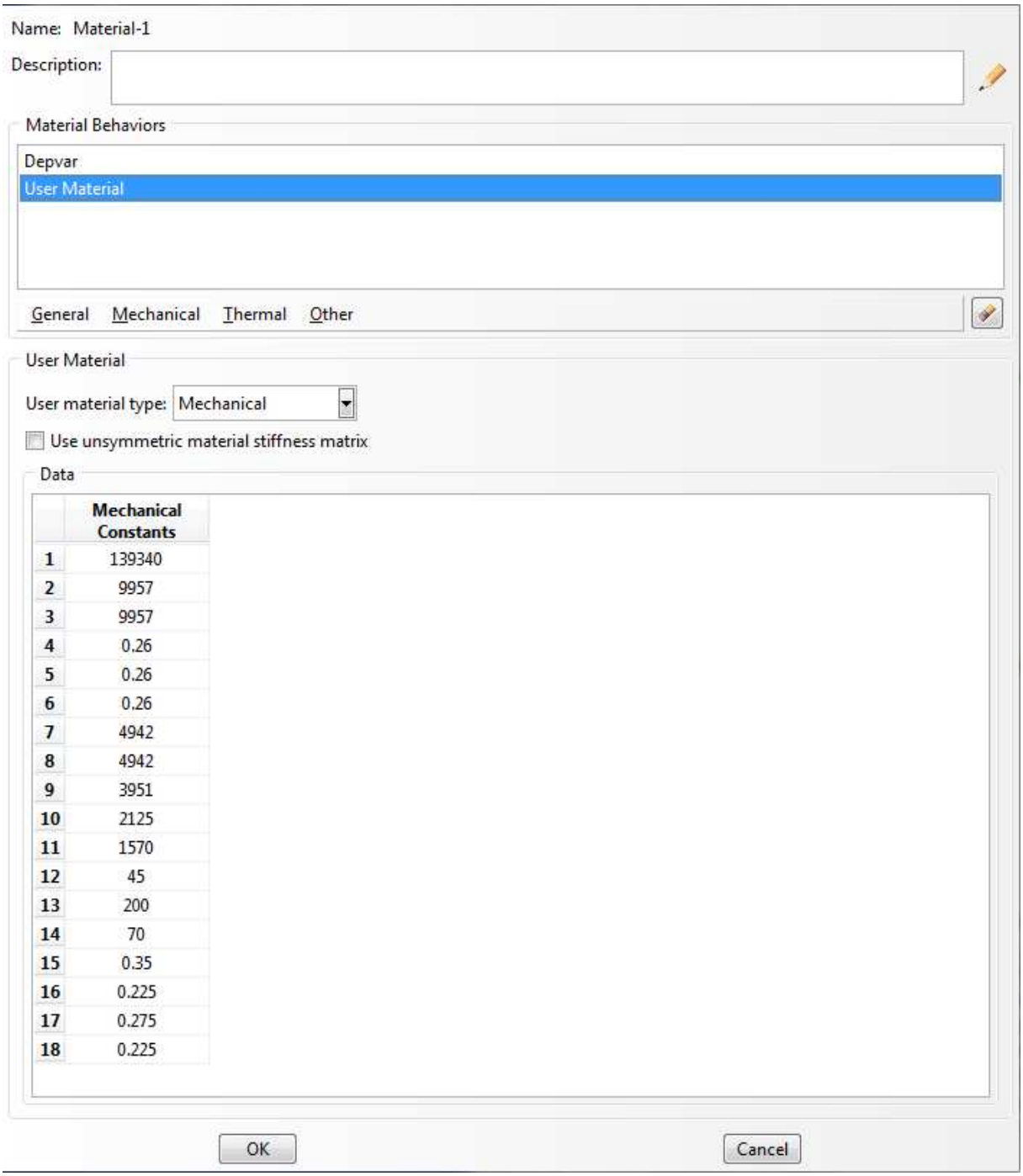

Figure 3-4 Material constants settings

COORDS- an array containing the coordinates of this integration point. These are the current coordinates if geometric nonlinearity is accounted for during the step, otherwise, the array contains the original coordinates of the point.

DFGRD0(3,3)- array containing the deformation gradient at the beginning of the increment. If a local orientation is defined at the material point, the deformation gradient components are expressed in the local coordinate system defined by the orientation at the beginning of the increment.

DFGRD1(3,3)- array containing the deformation gradient at the end of the increment. If a local orientation is defined at the material point, the deformation gradient components are expressed in the local coordinate system defined by the orientation. This array is set to the identity matrix if nonlinear geometric effects are not included in the step definition associated with this increment.

NOEL- this variable returns the number of element from the model.

NPT- this variable returns the number of integration point.

LAYER- layer number.

KSPT- section point number within the current layer.

KSTEP- step number.

KINC- increment number.

The whole process begins in Abaqus module, where a geometrical model has to be built and all material properties, boundary conditions and applied load are defined. It includes geometrical dimensions of the model, as well as composite layup and layup's coordinates systems. Then meshing properties such as number of elements, in which the model will be divided, and type of elements (including number of integration points for each element) must be provided in this part. Also here, material constants: Young's modulus, shear modulus, Poisson's ratios, strength resistances and slope parameters must be defined. This values are defined in Abaqus main program as mechanical constants. Every increment Abaqus main program stends this values to the UMAT subroutine where they are contained in the PROPS array. Then boundary conditions and loading for each step must be provided. The last step is setting the connection between Abaqus and UMAT subroutine. It has to be defined that Abaqus must use defined subroutine in every increment during the process of solving the model.

At the beginning of the solution, UMAT subroutine is provided with the strain at the beginning of the load increment and also all other properties mentioned above. On the bases of the orthotropic material law (see equations: 2.21-2.36), UMAT is calculating the elasticity matrix with the initial value of material constants (in the first increment material constants are not degraded yet) and then the particular state of stress on the basis of the input state of strain. From these stresses and material strength resistances, the fibre fracture $f_{E\,FF}$ is calculated (see equations: 2.2,2.3). After that, the stresses of the action plane $\sigma_n(\theta), \tau_{nt}(\theta), \tau_{n1}(\theta)$ are calculated for each action plane angle. Then the inter-fibre fracture stress exposure $f_{E\,IFF}$ is numerically calculated (see equations: 2.13,2.14) for numerous θ angle value to find the biggest value of this factor, as well as the θ angle for which it occurs. The calculated $f_{E\,FF}$ is then used to determine the weakening effect and weakening factor η_{w1} due to the fibre-parallel stress σ_1 influence. If the weakening occurs, then the result will be an increase of $f_{E\,IFF}$ value. If the IFF occurs then this value will be lower than 1. If the IFF does not occur, this value will be greater than 1 (or equal to 1, when the action plane strength resistance is reached). Then the subroutine procedure calculates residual stiffness fraction for Young's modulus and shear modulus (see equations: 2.44-2.45). This values will be equal to 1, if the $f_{E\,IFF}$ value is greater or equal to 1. This is the end of subroutine for current increment and all calculated and updated values (state of stresses, strains, Jacobian, IFF and residual stiffness fractions) are sent back to Abaqus. In the next increment, subroutine is provided with updated state of stress from previous increment and increment of strains at the current time-step. The material constants are multiply by residual stiffness fractions and a new elasticity matrix is calculated. If in the previous increment the IFF did not occur, then it will be the same matrix, as the initial elasticity matrix. Then the whole procedure is repeated.

The degradation process will last as long, as we defined it in main program. It depends on the user when and with what reasons, the degradation process will be stopped. It is adopted that the degradation process is completed when the stresses related to degraded elements of elasticity matrix will converge to constant values. The degradation flow-char is shown below (should be consider with Appendix.1.).

What must be mentioned also here, is the process of finding the solution of current increment. As was mentioned before and shown in Fig. 3-2, Abaqus is looking for the solution in the current increment on base of the information from previous one. In this case, to stresses (STRESS(i)) calculated on base of the old elasticity matrix (DDSDDE(i)) in the previous increment we are adding stresses calculated on base of new, degraded, matrix (DDSDDE(i)) and current strain increment (DSTRAN). Then the solution is wrong. We have to correlate this value in the manner shown below.

STRESS(i+1)=STRESS(i)+DDSDDE(i+1)*DSTRAN [3.48]

DSTRESS=STRESS(i+1)-DDSDDE(i+1)*(STRAN(i)+DSTRAN) [3.49]

STRESS(i+1)*=STRESS(i+1)-DSTRESS(i+1) [3.50]

where STRESS(i+1)* is our final solution.

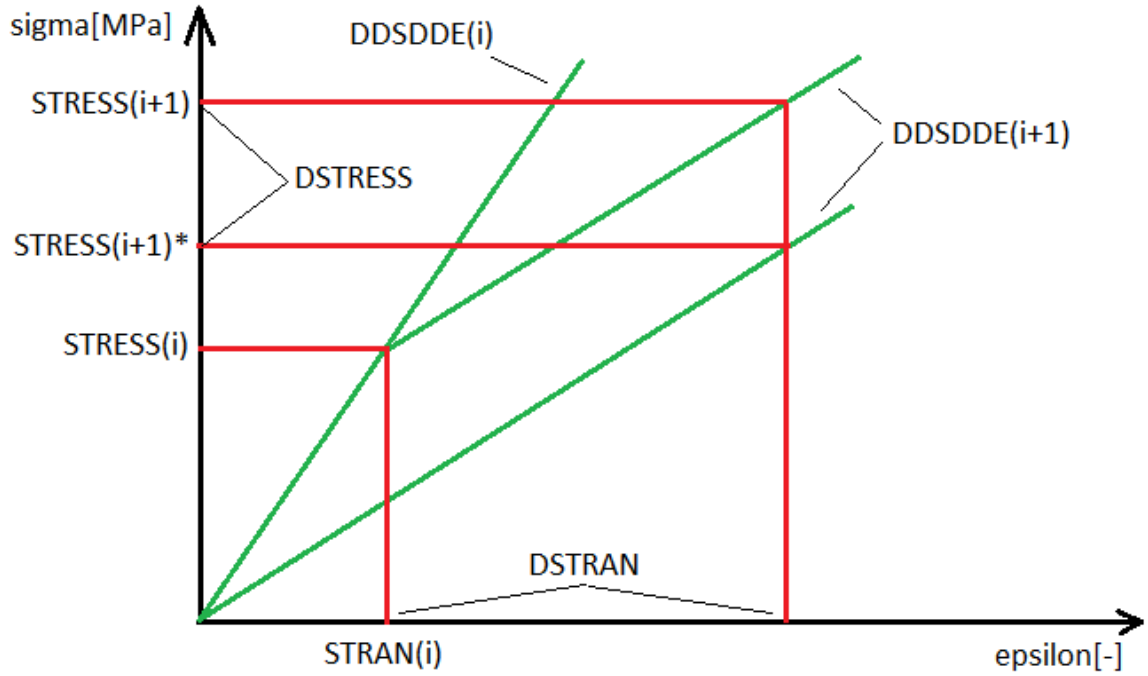

Figure 3-5 Solution finding process

Figure 3-5 shows how the finding proper solution is proceed.

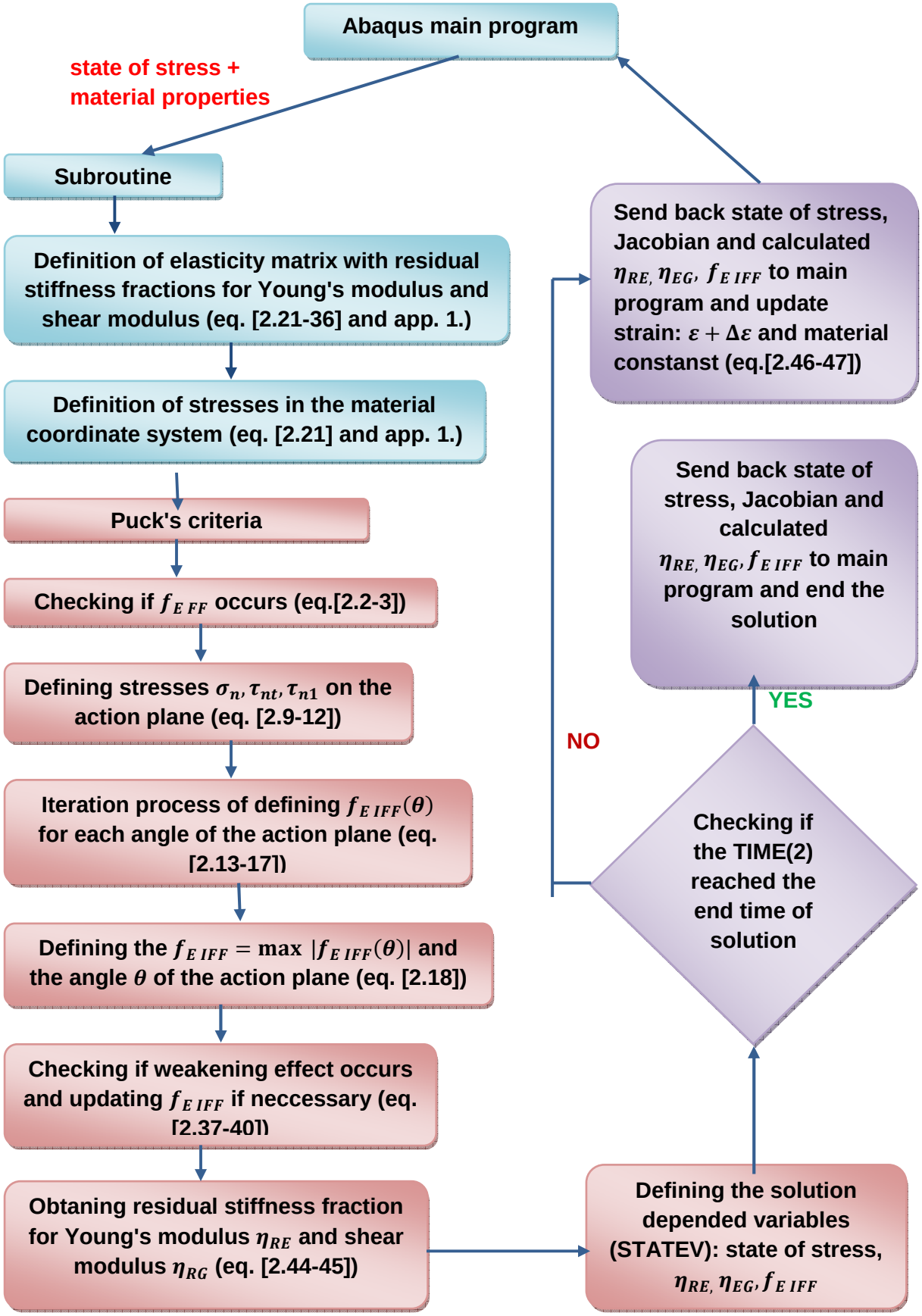

Figure 3-6 Scheme of degradation process

4. Experimental data and Compositor calculations

At the end of this thesis an implementation of the action plane fracture criteria of Puck into Abaqus software is provided. As was said before, the subroutine code will be prepared in Fortran and used in Abaqus CAE module. Nevertheless, this code, somehow, must be validated. The only reliable process to check, whether is it working properly, it is to compare it with experimental data and also with other calculation programme. In this chapter, one example of degradation process on the basis of some experimental researches (cp. Lit.3) and one own example will be provided and checked in Compositor. Both of them, will be examples of three-layer composite but with different layup and hence to that, different state of stress and strain is expected. This examples will be later used to validate Abaqus calculations. The results of experiments can be written in Lit.3.

As it was said at the beginning of this thesis, Compositor is an calculation spreadsheet prepared and developed by Instutut für Kunsttoffverarbeitung, RWTH Aachen. This program was specially prepared for Puck's criteria calculations for 2-dimensional models of lamina. In this program we can model a lamina and in base of classical laminate theory calculate the state of stresses and strains for an applied load. Then with the Puck's criteria module, we are able to check whether IFF occurs and define the value of IFF and residual stiffness fraction for Young's modulus and shear modulus.

4.1. Degradation of 3-layer lamina with 0°/90°/0° layers

In the first example, the degradation of Young's modulus transverse to the fibres $E_{\perp}$ and shear modulus $G_{\perp}$ was investigated using flat specimens. The laminate of the specimens was built up of a 5 mm thick test layer with the fibre direction 90°. This layer was supported with two 1 mm thick layer with fibre direction 0°. This kind of lamina is especially used for coefficients calibration. The only possible inter-fibre fracture can occur in the 90° layer and that is why it so easy to observe the degradation process. Tests were conducted on a hydraulic tension/compression machine. The laminate was loaded with a monotonously increasing tensile force in the direction of supporting layers fibres. Inter-fibre fracture was detected optically, acoustically and by sudden drop of stiffness. The test was stopped after IFF occurred. The laminate was unloaded and reloaded again until a new IFF occurred. This procedure was repeated until crack saturation was reached. Basing on state of stress and strains, fractures and degradations values were calculated. Material used in this example was Toray T700, Epoxy Vantico LY556/HY917/DY063 (cp. Lit.3.).

This test was repeated in Compositor. Obviously, as long as, the Compositor is an Excel calculation sheet, no time-depended calculation could be provided. In that case, a loading that causes inter-fibre fracture must have been guessed. Second thing that must be

mentioned is that Compositor is basing o 2D state of stress. Below Fig. 4-1 shows the boundary conditions and applied load.

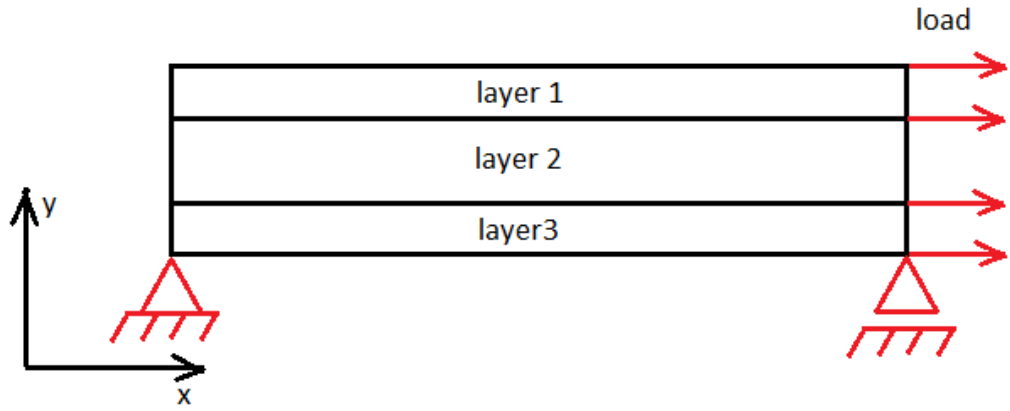

Figure 4-1 Sketch of loading and bundary conditions

Due to this fact, a procedure in Compositor is as it follows. The laminate is loaded with a constant, guessed value of load. Then the IFF criterion for test layer is checked and if IFF does not occur, the value of loading is increased and IFF is checked again. For the purpose of this calculations it set that IFF value should has the value around 1,01, which is equal to 1% of overstraining. This part of procedure is stopped when a suitable loading, causing IFF, is found.

When IFF occurs, then exposure factor is calculated and material constants, such as $E_{\perp}$ and $G_{\perp}$ are degraded. After that, a new stiffness matrix is calculated and the laminate is loaded again and the procedure of searching the load causing IFF is repeated. This iteration process is being continued until Young's transverse modulus, shear modulus and stresses converge to constant values.

On below Fig. 4-1 we can observe the degradation process of material constants in the 90° layer. The final value of shear modulus is 99,15% of the beginning value of this modulus. The final value of Young's modulus is 81,08% of the beginning value. Young's modulus has been degraded more than shear modulus which is correct with the theory provided in section 2.6. We can also observe that both modulus are decreasing almost linearly.

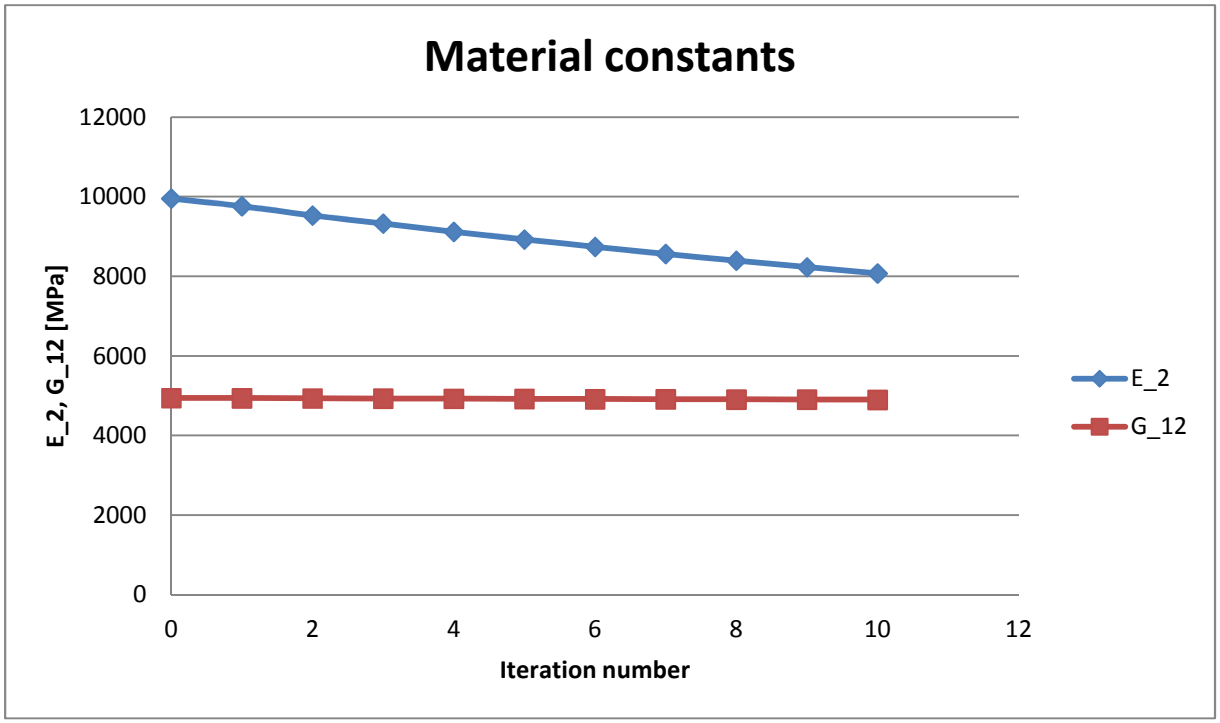

Figure 4-2 Material constants of 90 degree layer [see Ap.2]

During the process if searching the load causing IFF for every iteration, it occurs that value of this load increases almost linearly every iteration. It is due to the fact that the load applied in the previous iteration, cannot cause overstraining in the current iteration with the degraded material constants.

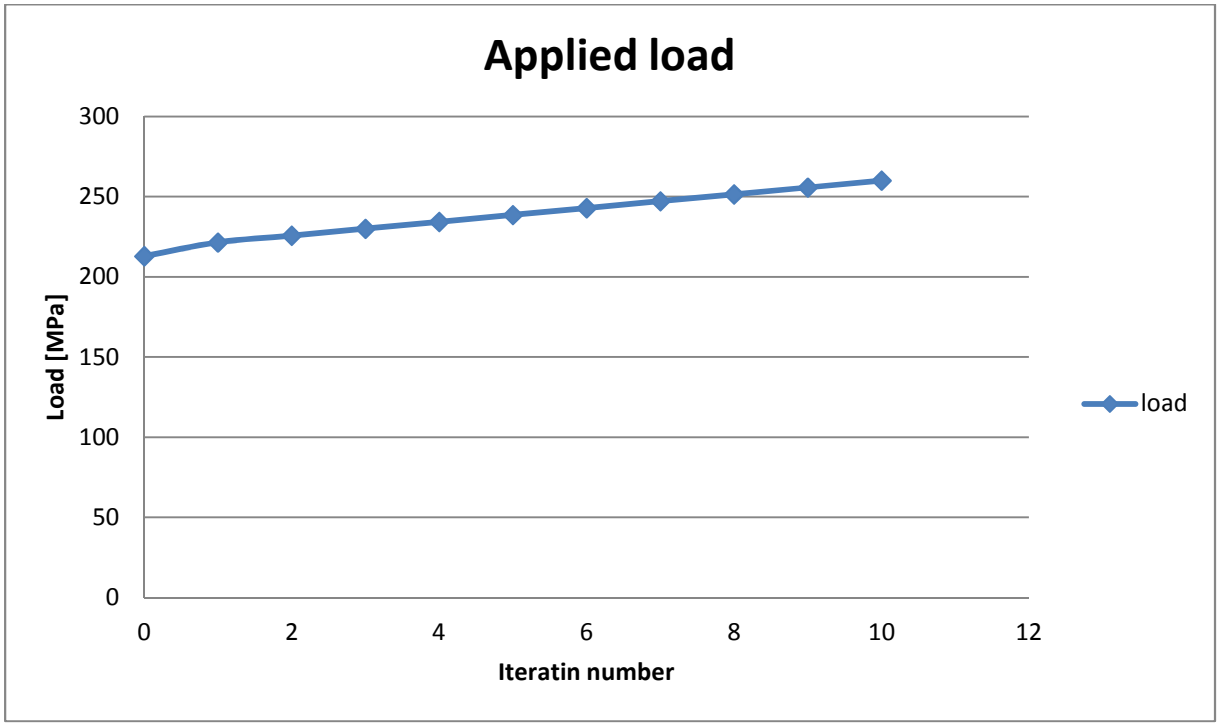

Figure 4-3 Applied load (cp. Appendix.2.)

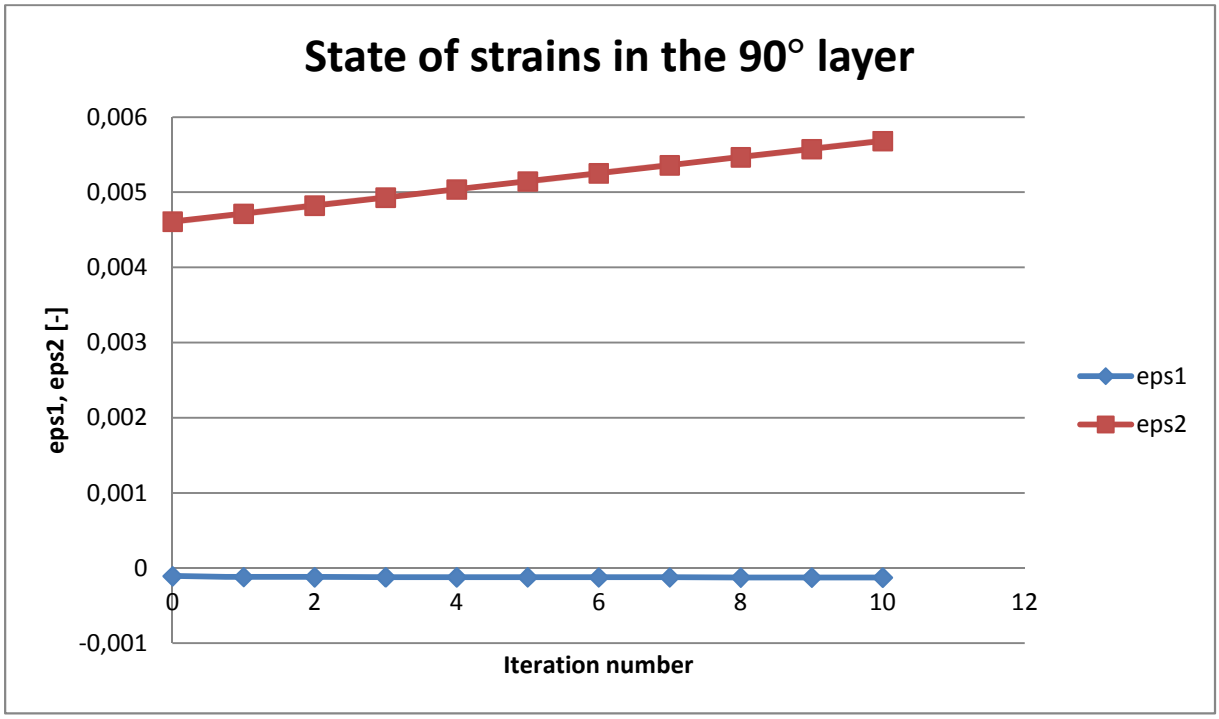

Figure 4-4 State of strains in the 90 degree layer (cp. Appendix.2.)

Figure 4-3 shows that during the degradation process strains in the 90° layer in the direction of applied load are increasing. Strains in the perpendicular direction stays about constant value during the degradation process.

Figures 4-4 and 4-5 show changing of states of stress in 90° and 0° layers. As we can observe stress σ_2 in the 90° layer converge to constant value after first three iterations and this layer is already degraded. In the figure 4-5 we can observe monotonously increasing stress σ_1 in the 0° layer. It means that additional load was carried by this layer, what also explains why the increase of strains ε_2 in the 90 layer, does not meaningfully influences on stresses in this layer.

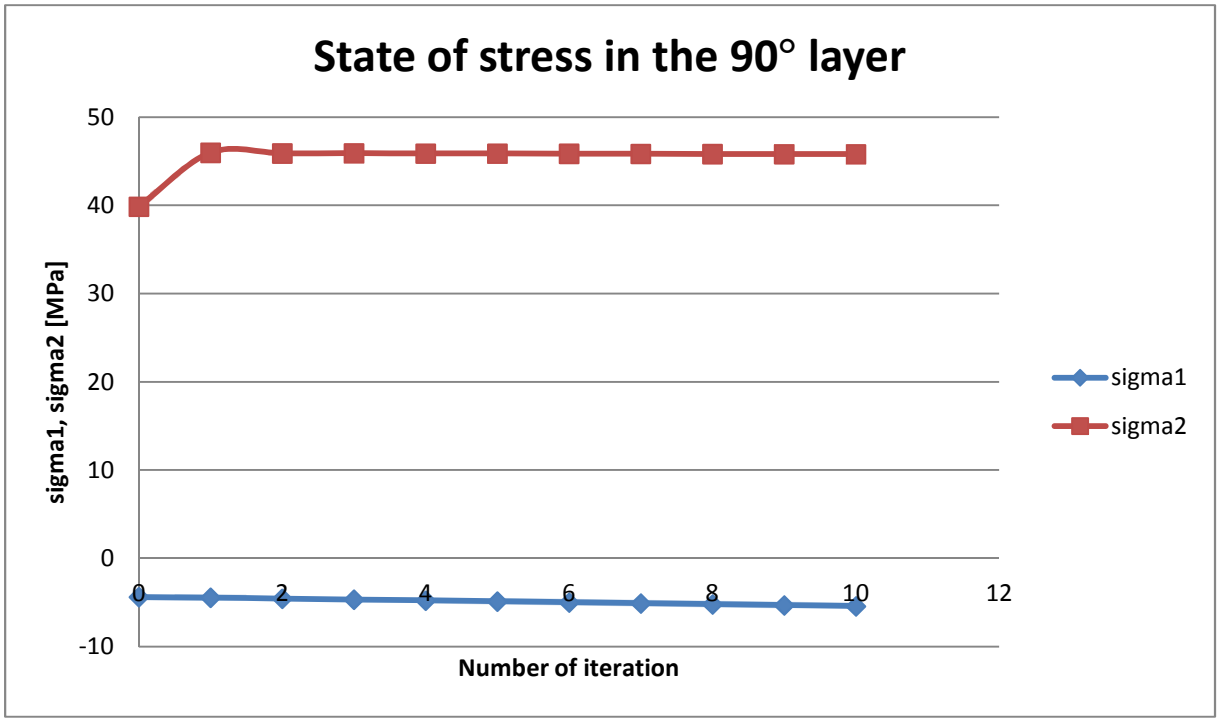

Figure 4-5 State of stress in the 90 degree layer (cp. Appendix.2.)

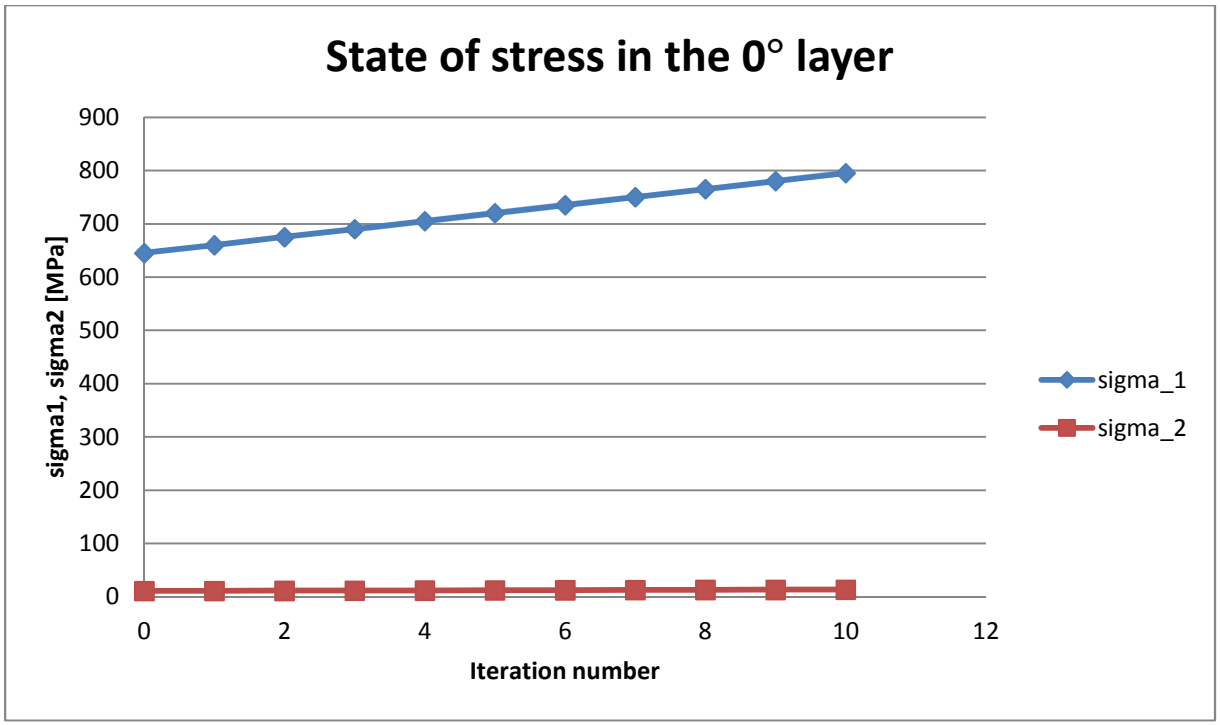

Figure 4-6 State of stress in the 0 degree layer (cp. Appendix.2.)

4.2. Degradation of 3-layer lamina with -45°/90°/-45° layers

In the second example, the whole Compositor procedure proceeded in the same way as in the first example. The difference was only the layup. In this case, the laminate of the specimens was built up of 3 mm thick test layer with the fibre direction 90°. This layer was supported with two 0,5 mm thick layer with fibre direction 45°. This change should cause some shearing stresses in test layer. In this example, in a comparison to the previous, inter-fibre fracture can also occur in the supporting layers.

Below figures 4-6 and 4-7 show material constant degradation. In comparison to the previous example, we can observe here, that after five iteration the inter-fibre fracture of supporting layers (-45°) occurs. It is due to the fact that fibre direction of supporting layer is not parallel to the load direction and increasing load made impact also on this layer.

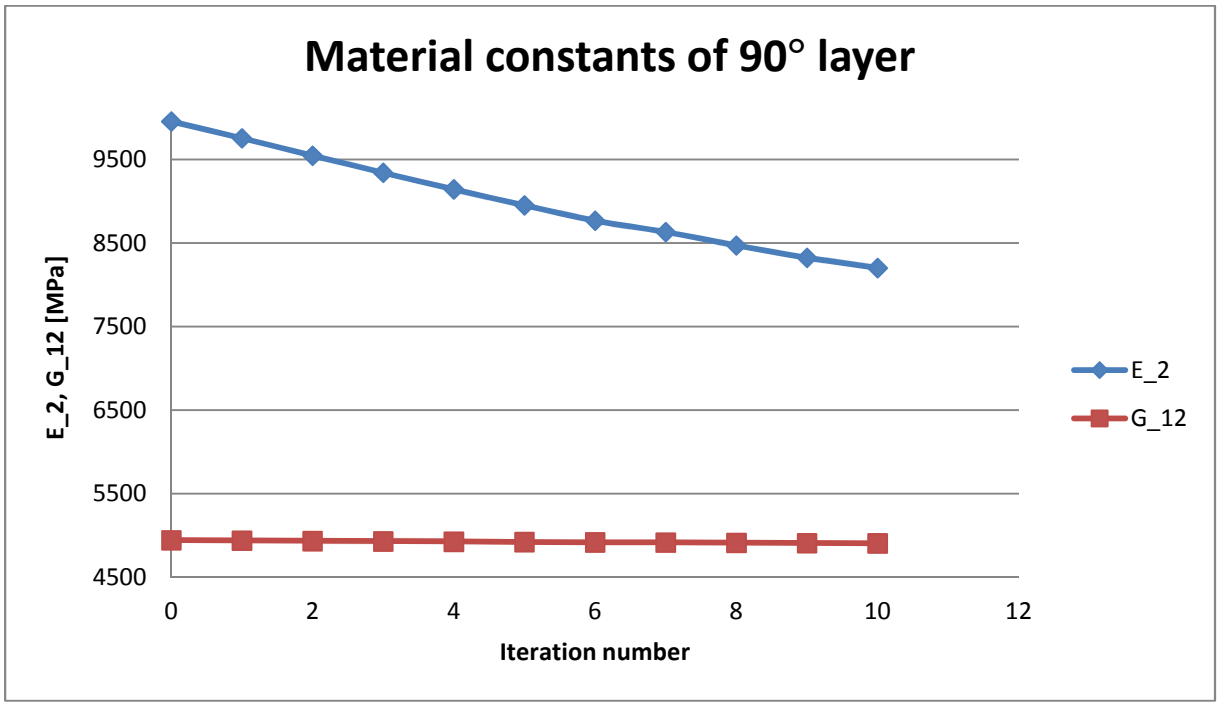

Figure 4-7 Material constants of 90 degree layer (cp. Appendix.3.)

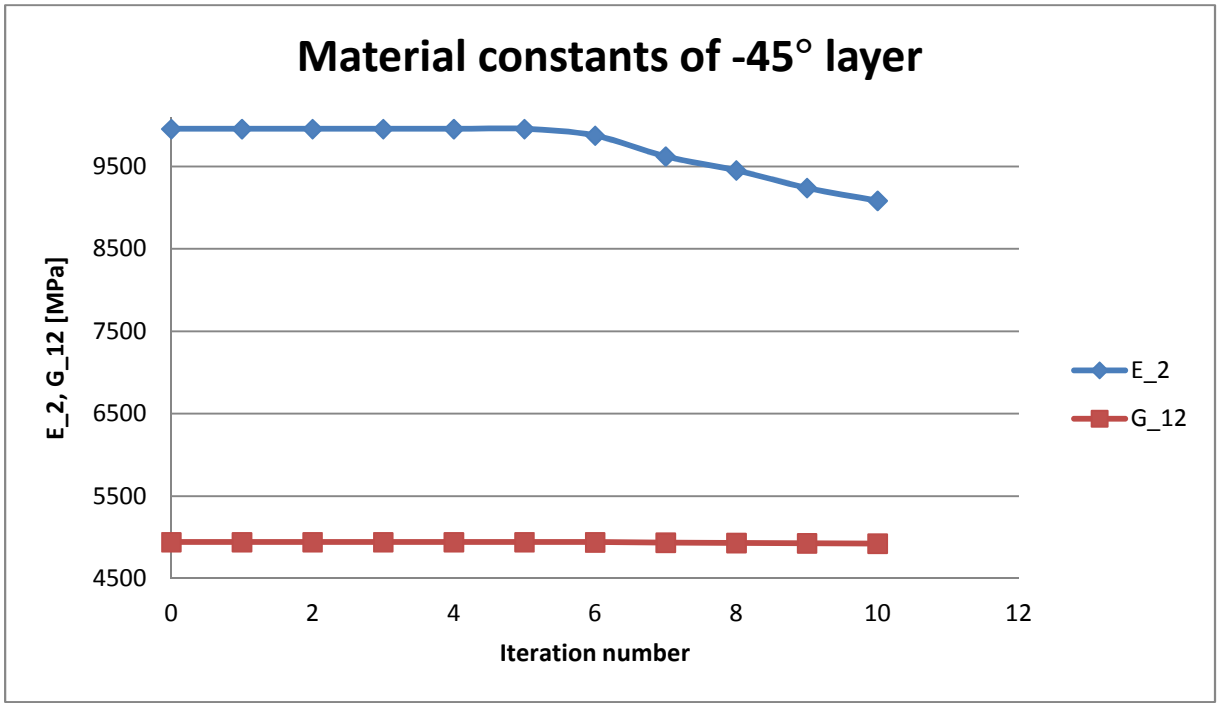

Figure 4-8 Material constants of -45 degree layer (cp. Appendix.3.)

As the consequence of the fact of degradation in every layer, the load-carrying capability of whole lamina is decreasing. Hence the applied load which causes IFF converging to constant value (see Fig.[4-8]). It means that every iteration, the increment of load needed to cause fracture in degraded lamina is getting lower.

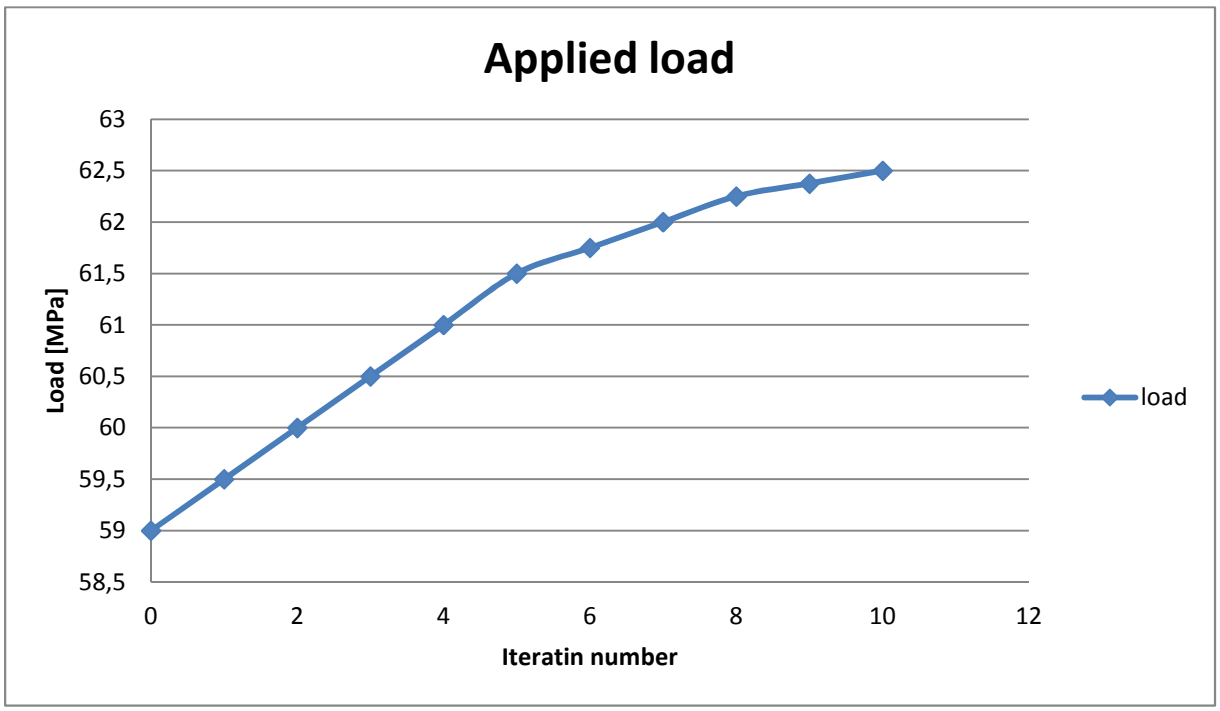

Figure 4-9 Applied load (cp. Appendix.3.)

As we can observe on below figures 4-9 and 4-10, there is a difference between state of stress in this example and the previous one (see section 4.1). First of all, because of non-parallel fibre direction in supporting layer, shear stresses appeared in the lamina. Due to the fact that in every layer an IFF occurs, and additional load cannot be carried by supporting layers. We can observe that in 90° layer stresses σ_2 are constant from the beginning. Stresses σ_1 and τ_{12} are also converging to constant value. The differences between staring and final value for these stresses are small. In the 0° layer the stresses σ_1 are increasing before the first fracture appears and the start to converge to constant value. Stresses σ_2 and τ_{12} very quickly converged to constant value.

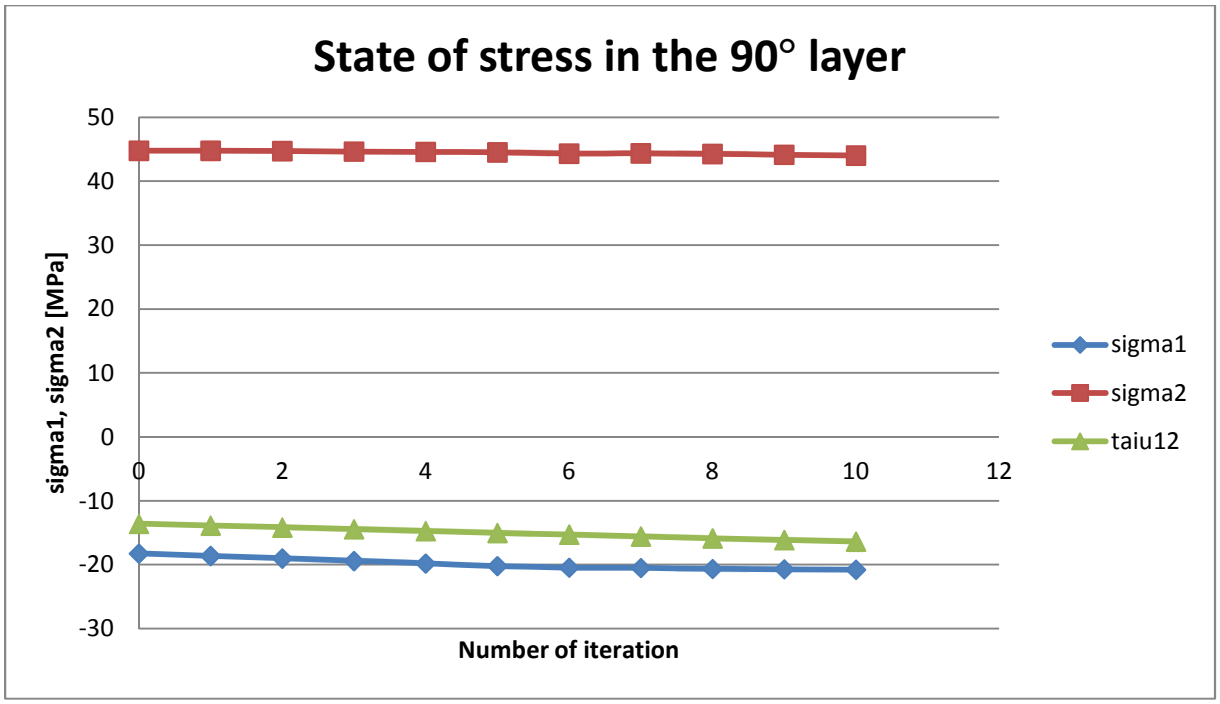

Figure 4-10 State of stress in the 90 degree layer (cp. Appendix.3.)

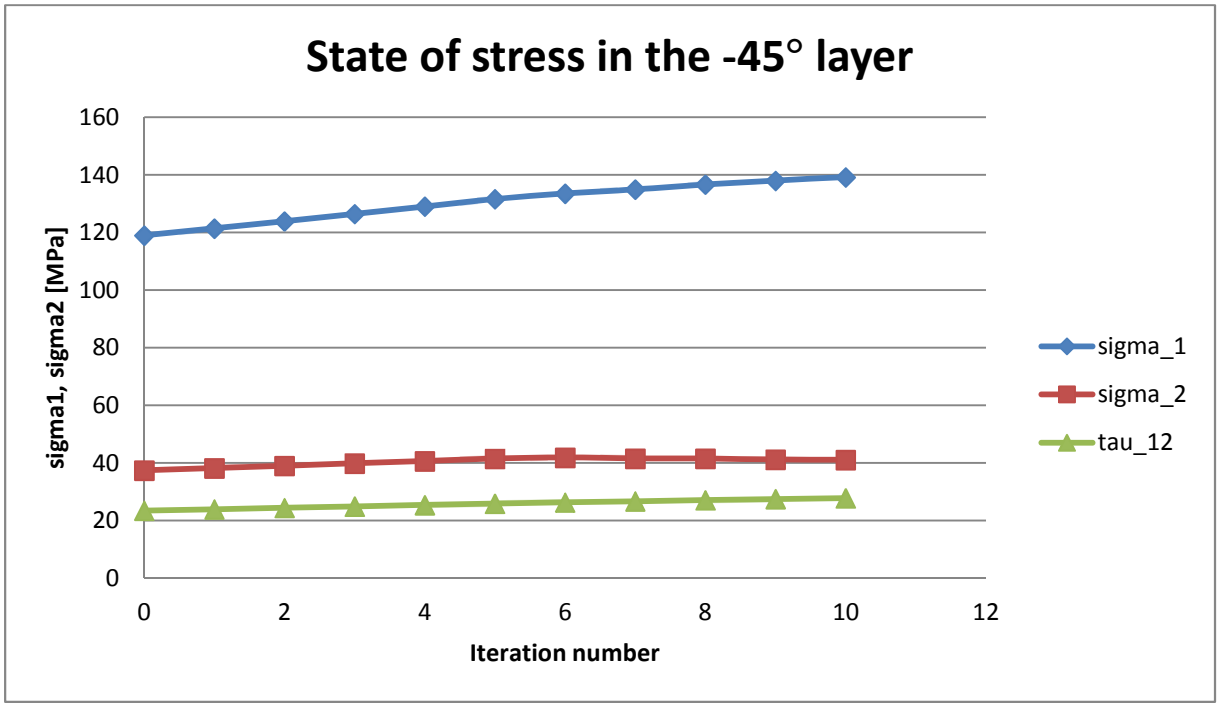

Figure 4-11 State of stress in the 0 -45 degree layae (cp. Appendix.3.)

5. Abaqus Cae standard

Before there is a possibility to implement the Puck's criteria into Abaqus, there is a need to check whether Abaqus CAE mode is properly calculating states of strain and stress with applied load. It will be validate with simple examples, that can be checked with manual calculation. First for 2D state of stress and then for 3D state of stress, both for isotropic materials. This step is very important, cause thanks to that, we can be sure that the only errors that can occurs, are caused by wrong implementation and it will help to find errors and fix them.

5.1. 2D state of stress

The first calculated example will be a 2-dimensional state of stress. The model was a 4-node, square plate element of dimensions 1mm x 1mm with boundary as shown below:

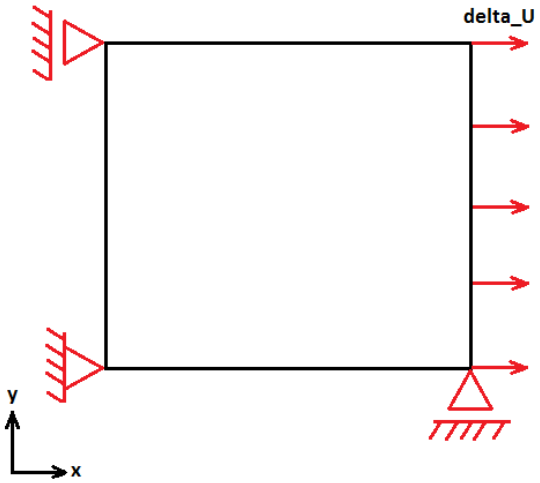

Figure 5-1 2D model and boundary conditions

The material of the model was steel with material constants value E=210 000 MPa and Poisson's ratio equal to 0.3. The applied displacement Δu=0.01mm.

First manual calculations will be shown and then compared with results from Abaqus software.

$$\varepsilon_x = \frac{\Delta u_x}{u_x} = \frac{0.01}{1} = 0.01$$

$$\varepsilon_y = -\nu * \varepsilon_x = -0.3 * 0.01 = -0.003$$

$$\Delta u_y = u_y * \varepsilon_y = -0.003\ [mm]$$

$$\sigma_x = \varepsilon * E = 0.01 * 2.1 * 10^5 = 2.1 * 10^3 [MPa]$$

$$\sigma_y = \frac{E}{1-\upsilon^2}\left(\varepsilon_y - \upsilon * \varepsilon_x\right) = 0\ [MPa]$$

Obviously in such case, stresses will have constant value in whole model. Actually, there was no need to calculate stresses in the Y-direction, because there is no contraction in this direction, but this equation also proves it.

Results provided by Abaqus for this example were the same. It proves that in 2D dimensional state of stress, for isotropic material model, Abaqus provides proper results.

5.2. 3D state of stress

Now whole procedure, as shown in previous chapter, will be repeated, but for 3-dimensional example. The model now will be one, 8-node, hexagonal element with following dimensions: 1mm x 1mm x 1mm. Boundary conditions in 0XY surface will stay the same as in 2D example. The only change is an additional boundary on 0Z direction, shown below [Fig.5-6].

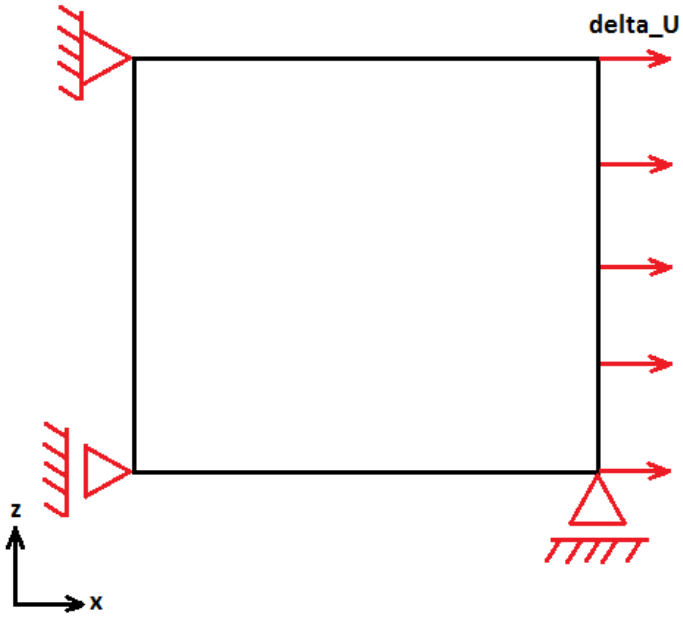

Figure 5-2 0XZ boundaray conditions for 3D model

The material of the model was steel with material constants value E=210 000 MPa and Poisson's ratio equal to 0.3. The applied displacement Δu=0.01mm.

As before, first manual calculations will be provided.

$$\varepsilon_x = \frac{\Delta u_x}{u_x} = \frac{0.01}{1} = 0.01$$

$$\sigma_x = \varepsilon * E = 0.01 * 2.1 * 10^5 = 2.1 * 10^3 [MPa]$$

There is no contraction in 0Y and 0Z directions, therefore we can assume that stresses in these directions are equal to zero.

$$\sigma_y = \sigma_z = 0$$

That's why we are able to write following equations:

$$\varepsilon_y = \frac{1}{E}\left[\sigma_y - \upsilon * (\sigma_z + \sigma_x)\right] = \frac{-\upsilon * \sigma_x}{E}$$

$$\varepsilon_y = \frac{1}{E}\left[\sigma_z - \upsilon * \left(\sigma_x + \sigma_y\right)\right] = \frac{-\upsilon * \sigma_x}{E}$$

$$\varepsilon_y = \varepsilon_z = -0.003$$

$$\Delta u_y = \Delta u_z = u_y * \varepsilon_y = u_z * \varepsilon_z = -0.003\ [mm]$$

Results from Abaqus gives us the the same displacement values and stresse as calculated manually. Only for stresses σ_y, σ_z we can notice that values are not exactly zero, but the values are negligibly small (~10^{-13}) and we can assume them as numerical errors and recognize them as zeros.

All in all, above calculations prove that Abaqus CAE module is providing proper values for state of stress and strains, for 2-dimensional state, as well as for 3-dimensional.

What is more, we can see that results from 2-dimensional model with 3-dimensional model. This is very important for the comparison results from Abaqus with Compositor calculation. There is a wish to compare 2-dimensional model of lamina, calculated in Compositor with 3-dimensional model created in Abaqus. Thanks to above calculation we are sure that it is possible with proper boundary conditions.

6. Comparison between Abaqus and Compositor results

In this section it will provided the comparison between results of degradation process of lamina on base of Compositor calculations and results gained from Abaqus with the usage of user-subroutine UMAT.

To do such comparison, the model in Abaqus must be properly prepared first. As we showed in the section 5, it is possible to compare 2-dimensional and 3-dimensional solution. As far as subroutine UMAT is delived for 3-dimensional state of stress and strain, we have to modify material constants to achieve solution comparable with 2-dimensial state of stress and strain. For this reason no stresses in the Z direction can occurs due to contraction. It is achieved by setting Poisson's values $\upsilon_{13}, \upsilon_{23}$ to zeros. In this manner the elasticity matrix is simplified to equation. 6.50.

$$\begin{bmatrix} \sigma_1 \\ \sigma_2 \\ \sigma_3 \\ \tau_{12} \\ \tau_{13} \\ \tau_{23} \end{bmatrix} = \begin{bmatrix} D_{1111} & D_{1122} & 0 & 0 & 0 & 0 \\ D_{2211} & D_{2222} & 0 & 0 & 0 & 0 \\ 0 & 0 & 0 & 0 & 0 & 0 \\ 0 & 0 & 0 & D_{1212} & 0 & 0 \\ 0 & 0 & 0 & 0 & D_{1313} & 0 \\ 0 & 0 & 0 & 0 & 0 & D_{2323} \end{bmatrix} * \begin{bmatrix} \varepsilon_1 \\ \varepsilon_2 \\ \varepsilon_3 \\ \gamma_{12} \\ \gamma_{13} \\ \gamma_{23} \end{bmatrix} \qquad [6.51]$$

Moreover it is better to applied displacement in Abaqus than the load. Thanks to that we can achieve in Abaqus almost exact state of strain as in Compositor. The procedure was to applied the displacement provided by Compositor in the direction of applied load.

Proper boundary are also needed. To achieve the same values we have to define boundary conditions working in the same manner in Compositor (cp. Fig.4-1) and in Abaqus. This boundary condition will be the same as shown in Fig. 5-1 and 5-2.

6.1. Abaqus results for example from section 4-1

In the section 4-1 it is shown that only in the 90° layer an IFF occured. Also in Abaqus no IFF occurs in 0° layers. Due to this fact is it not necessary to compare results for material constants and IFF for 0° layers. For these layers only state of stress is compared.

As long as Abaqus model is divide into several number of elements, it is not possible to achieve one constant value for whole layer. It is also due to the fact that in Abaqus model the constraints and reaction between each layers is taken into account. Then a range of values is achieved in dependency of the position of each degradation point. The comparison is recognized as a successful when a value from Compositor is included in the range of values from Abaqus.

Table 6-1 shows value of IFF achieved in Compositor and Abaqus. As we can see, for every step value from Compositor is included in the range of values from Abaqus. In this table we can also see the difference in percents between values from Compositor and values from Abaqus in the middle of the layer.

IFF				
Step nr	Compositor	Abaqus	Abaqus values in the middle of layer	Delta[%]
1	1,01684	1,01-1,017	1,015	0,18083
2	1,01684	1,015-1,021	1,016	0,08248
3	1,01540	1,012-1,017	1,016	0,05923
4	1,01578	1,014-1,019	1,015	0,07643
5	1,01514	1,012-1,016	1,015	0,01367
6	1,01512	1,014-1,017	1,015	0,01203
7	1,01472	1,013-1,016	1,015	0,02793
8	1,01468	1,014-1,016	1,014	0,06731
9	1,01433	1,013-1,015	1,014	0,03233
10	1,01411	1,013-1,015	1,014	0,01044
11	1,01399	1,013-1,014	1,014	0,00100

Table 6-1 Comparison of IFF in 90 degree layer for 0/90/0 layup

In Fig. 6-1 IFF is shown for the last step.

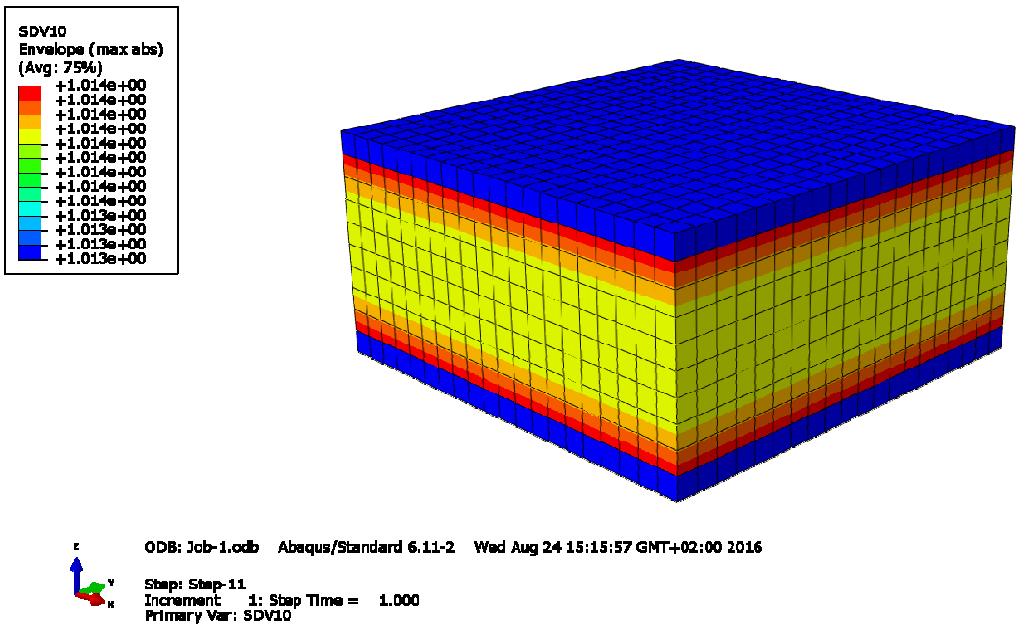

Figure 6-1 IFF for 90 degree layer in the 0/90/0 layup

Table 6-2 the σ_1 stresses for each step. Values are provided as absolute values. Here we can observe that the range of values gained from Abaqus is quite big, is due to the fact of

contraction in Y direction between layers. The influence of this reaction increases getting closer to the border of the layer, where stresses are the bigger. Nevertheless, values from Compositor are included in the range of values from Abaqus. For the middle of the layer the values are converged to the smallest value from the range. Therefore, the difference is really big around 95%.

sigma_1 [MPa]		
Step nr	Compositor	Abaqus (absolute values)
1	4,374783777	0,1229-13,8
2	4,43702505	0,147-14,08
3	4,547218057	0,134-14,42
4	4,655241499	0,125-14,72
5	4,764456482	0,117-15,04
6	4,872974874	0,1145-15,36
7	4,981888668	0,114-15,67
8	5,090518353	0,1145-16,01
9	5,199394124	0,142-16,32
10	5,308024384	0,146-16,66
11	5,416713396	0,1145-16,98

Table 6-2 Comparison of sigma_1 stress in 90 degree layer in 0/90/0 layup

In Fig. 6-1σ_1 is shown for the last step.

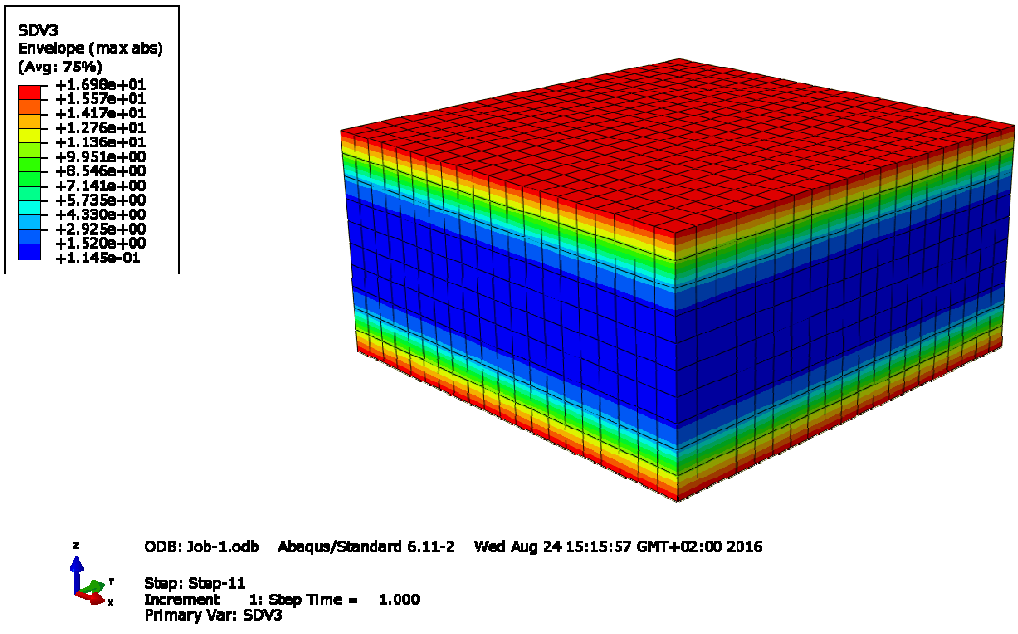

Figure 6-2 Sigma_1 stress for 90 degree layer in the 0/90/0 layup

In the table 6-3 we can observe that the value stress σ_2 gained from Compositor is almost always bigger than the range of values obtained with Abaqus. However, the

difference is about 0,5% what is acceptable. There is only a bigger difference in the first. One of the reason might be the problem with procedure shown in equations 4.47-4.49 for the first stop. Another option is that some numerical problems occurs. In this figure it is also shown the difference in percents between value of stresses from Compositor and value of stresses from Abaqus in the middle of the 90° layer.

sigma_2 [MPa]				
Step nr	Compositor	Abaqus (absolute values)	Abaqus values in the middle of layer	Delta[%]
1	44,93451423	45,43-45,78	45,69	1,6535
2	45,97491627	45,67-45,93	45,74	0,5136
3	45,9032592	45,52-45,77	45,7	0,4448
4	45,9173934	45,64-45,84	45,7	0,4757
5	45,88441044	45,56-45,74	45,69	0,4255
6	45,87897279	45,63-45,78	45,67	0,4576
7	45,85789975	45,58-45,70	45,67	0,4114
8	45,84806127	45,62-45,72	45,65	0,4339
9	45,82849176	45,62-45,72	45,65	0,3910
10	45,81863054	45,61-45,68	45,63	0,4134
11	45,80644609	45,59-45,64	45,63	0,3867

Table 6-3 Comparison of sigma_2 stress in 90 degree layer in 0/90/0 layup

In Fig. 6-1σ_2 is shown for the last step.

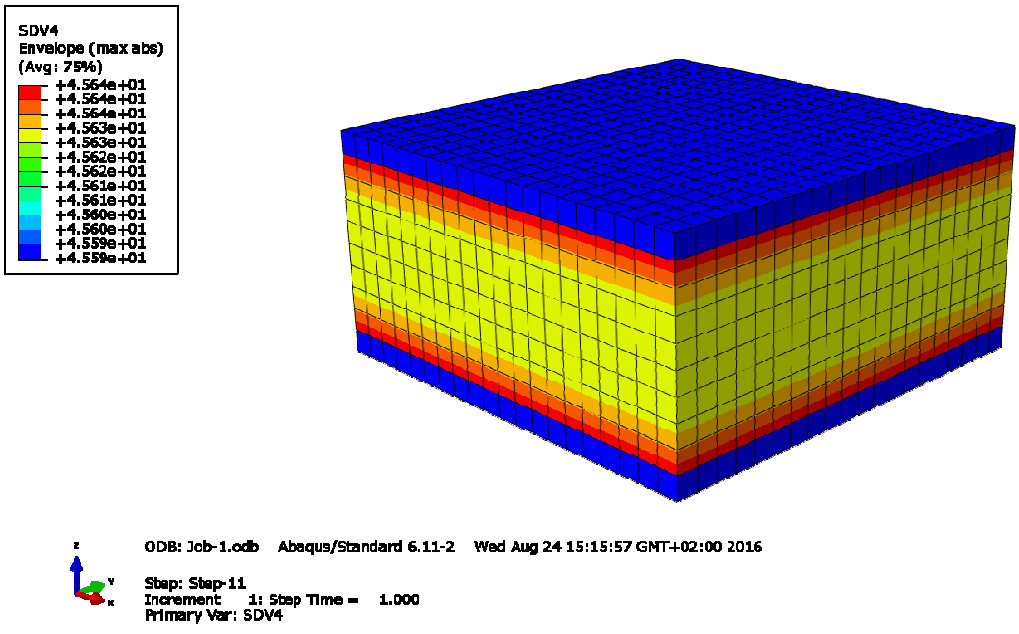

Figure 6-3 Sigma_2 stress for 90 degree layer in the 0/90/0 layup

As the last the comparison between material constants is provided. In the table 6-4 and 6-5 we can see that in all steps and for both values, the value from Compositor is

included in the range of values from Abaqus. In this figure it is also shown the difference in percents between value of material constants from Compositor and value of stresses from Abaqus in the middle of the 90° layer.

E_2 [MPa]				
Step nr	Compositor	Abaqus	Abaqus values in the middle of layer	Delta[%]
1	9765,092292	9709-9842	9744	0,21600
2	9530,804832	9512-9533	9516	0,15534
3	9327,124065	9279-9391	9308	0,20504
4	9121,197635	9099-9133	9106	0,16662
5	8930,102522	8888-8984	8913	0,19152
6	8743,363084	8719-8762	8729	0,16427
7	8566,530992	8529-8613	8550	0,19297
8	8394,589881	8370-8418	8381	0,16189
9	8231,275993	8198-8272	8216	0,18558
10	8073,660677	8048-8099	8060	0,16920
11	7921,290309	7891-7958	7907	0,18040

Table 6-4 Comparison of E_2 in 90 degree layer in 0/90/0 layup

In Fig. 6-1 E_2 is shown for the last step.

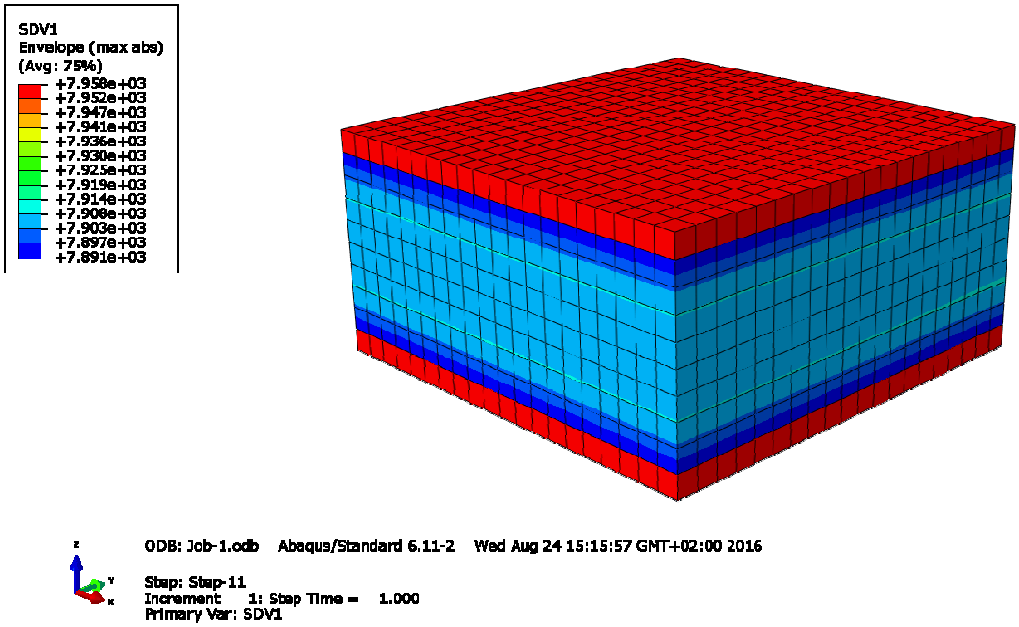

Figure 6-4 Young's modulus for 90 degree layer in the 0/90/0 layup

.

G_12[MPa]				
Step nr	Compositor	Abaqus	Abaqus values in the middle of layer	Delta[%]
1	4938,141147	4937-4940	4938	0,0029
2	4932,995315	4933-4933	4933	0,0001
3	4928,638833	4928-4930	4928	0,0130
4	4924,477936	4924-4924	4924	0,0097
5	4919,758533	4919-4921	4920	0,0049
6	4915,769089	4915-4916	4915	0,0156
7	4911,94456	4911-4913	4911	0,0192
8	4907,961997	4907-4908	4907	0,0196
9	4904,113446	4903-4905	4903	0,0227
10	4900,208198	4899-4900	4900	0,0042
11	4896,258818	4895-4897	4896	0,0053

Table 6-5 Comparison of G_12 in 90 degree layer in 0/90/0 layup

In Fig. 6-1 G_{12} is shown for the last step.

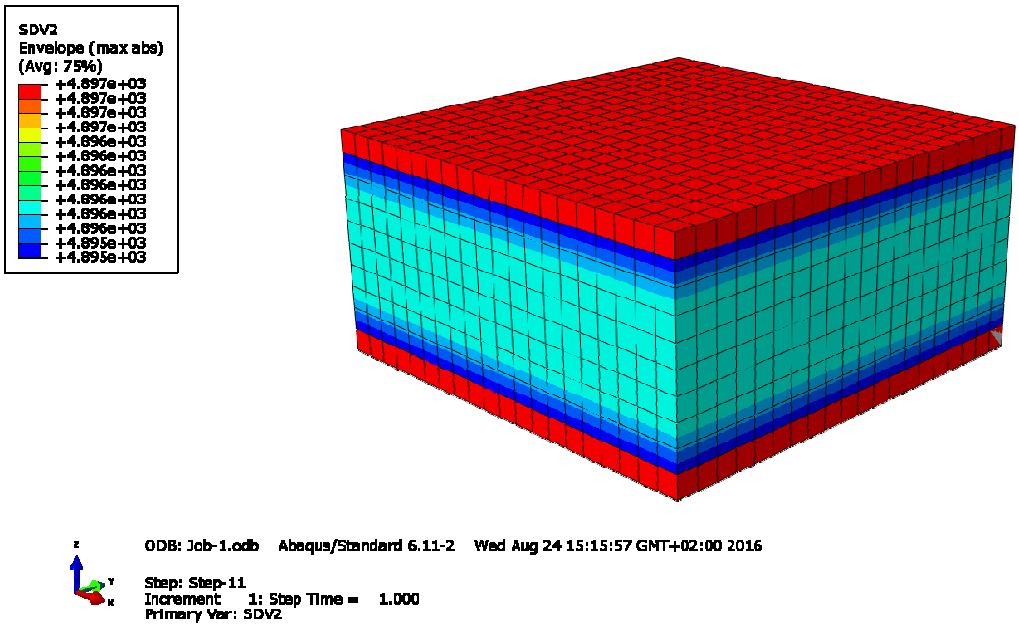

Figure 6-5 Shear modulus for 90 degree layer in the 0/90/0 layup

Considering above results we can come to the conclusion that, in this particular example, Abaqus provides results with the difference below 0,5% in comparison to results gained from Abaqus. This difference is calculated for values provided by Abaqus for the middle of the 90° layer, where the contraction in Y is the lower. This contraction is cause by interaction between layers in the Y direction. In the 2-dimensional state of stress on base of the Compositor, this contraction does not exist. In the 3-dimensional Abaqus model we cannot turn off this contraction. Because of this contraction there is also a big difference in σ_1 values between Compositor calculations and values achieved in Abaqus for the middle of the layer. Nevertheless, this difference in stresses σ_1 does not influence meaningfully on our results and our calculations look really promisingly.

6.2. Abaqus results for example from section 4-2

In the manner as in section 6-1, there was a wish to discuss the comparison between the Compositor results and results provide by Abaqus. Nevertheless, it turn out that choosing an example where shear stresses appears due to non parallel direction of fibre in the supporting layer do not give a suitable result in Abaqus that can be compare. Due to the fact that state of stress in laminas is not laminar, there is no opportunity to find suitable values to compare. Below Fig. 6-6 shows the stress σ_2.

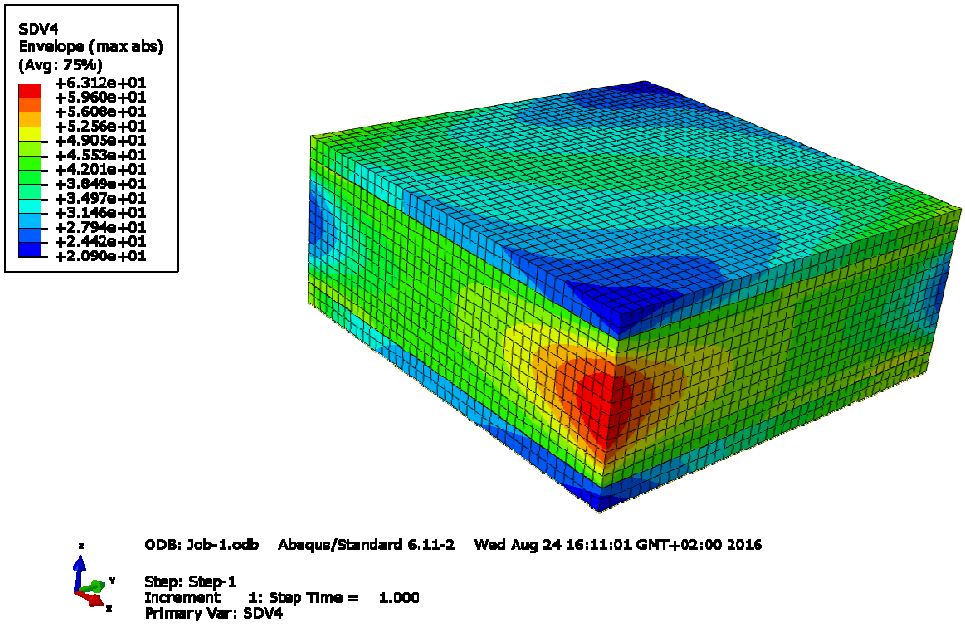

Figure 6-6 Sigma_2 stresess in the 45/90/45 lamina

To clarify it better, why there is no possibility of validate the calculation on base of Compositor, the Fig. 6-7 is shown. It shows the IFF for the first step. As we can see, in zones where big concentration of stress appears, we also achieve high IFF. On the other hand we also achieve zones where IFF is lower than one. In the end we have a big range of values (0,5676-1,403). In comparison, the Compositor gives as the IFF value equal to 1,01474. Of course this value is in the range of values gained from Abaqus, where maximum over-straining is about 40%. Nevertheless, on the basis on this we cannot validate if this is the same what Compositor gives.

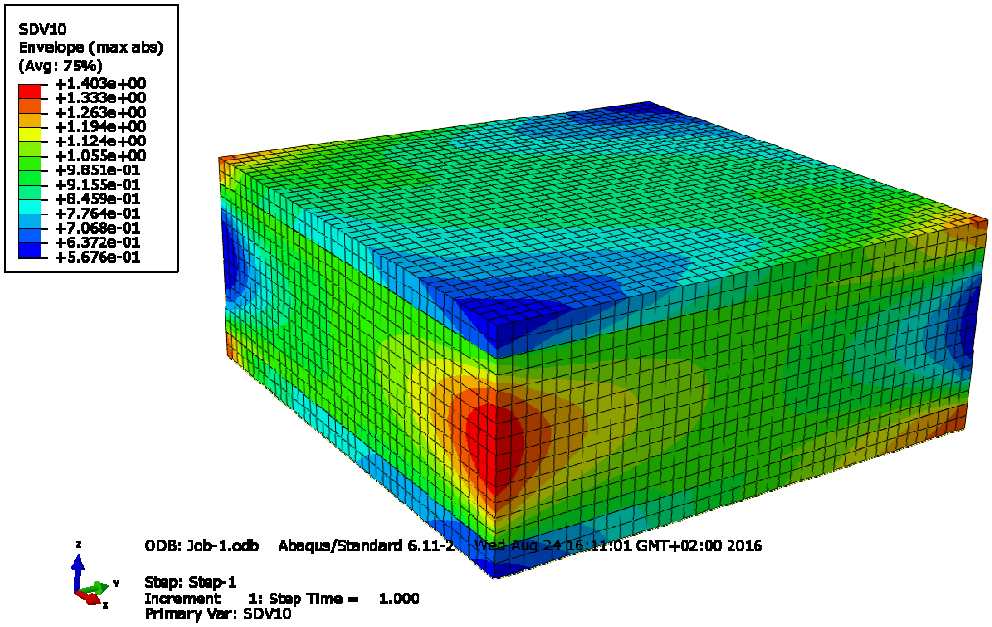

Figure 6-7 IFF in the 45/90/45 lamina

The first conclusion about this example was that supporting layer for flat specimens cannot has fibre orientation other than zero and only test layers can be orientated differently. To find out if this is the right thinking, number of examples were provide in Abaqus for different lamina's layup.

Example 1: 0⁄+-45⁄0 °

Example 2: 0⁄+-60⁄0 °

Example 3: 0⁄+-45° /90⁄+-45⁄0°

Unfortunately non of these examples is suitable to compare with results gained from Compositor. In non of these examples there is a zone of laminar state of stress, which allow us to compare a specific value of IFF, stresses or material constants. This shows that the only option to validate Puck's criteria on base of comparison with results from Compositor for flat specimens of lamina are laminas with only 0° and 90 ° degrees layer.

One of the opportunity to create a model, with other orientations of fibre, which can be compared is to create a model of a tube. Then this kind of model should be loaded in the direction of 0° axis or a torsion should be applied to the tube.

6.3. Abaqus results for example from section 4-2 for 3-dimensional state of stress

In the section 4-1 it is shown that Abaqus provides good results in comparison to 2-dimensional calculations of Compositor. Now the calculation for 3-dimensional state of stress, where also the contraction in Z direction will be taken into account, will be provided.

There is a wish to check how big influence will have the contraction in Z direction in this particular example of lamina. Therefore, results from Abaqus for the case from section 6-1 will be compared with results from Abaqus for the same example but with possibility of contraction in the Z direction. For simplification, in tables there are used abbreviations: Z-no for the model with no contraction in the Z direction and Z-yes for the model with possible contraction in the Z direction.

What we can observe in the table 6-6, is that generally we achieved the same inter-fibre fracture in both cases. Only in two steps we can find differences in the value of IFF for the middle of the layer, but they are smaller than 0,1%.

IFF					
Step nr	Abaqus (Z-no)	Abaqus values in the middle of layer (Z-no)	Abaqus (Z-yes)	Abaqus values in the middle of layer (Z-yes)	Delta[%]
1	1,01-1,017	1,015	1,01-1,017	1,015	0
2	1,015-1,021	1,016	1,015-1,021	1,017	0,098425
3	1,012-1,017	1,016	1,012-1,017	1,016	0
4	1,014-1,019	1,015	1,014-1,019	1,016	0,098522
5	1,012-1,016	1,015	1,012-1,016	1,015	0
6	1,014-1,017	1,015	1,014-1,017	1,015	0
7	1,013-1,016	1,015	1,013-1,016	1,015	0
8	1,014-1,016	1,014	1,014-1,016	1,014	0
9	1,013-1,015	1,014	1,013-1,015	1,014	0
10	1,013-1,015	1,014	1,014-1,015	1,014	0
11	1,013-1,014	1,014	1,013-1,014	1,014	0

Table 6-6 IFF comparison between two Abaqus models

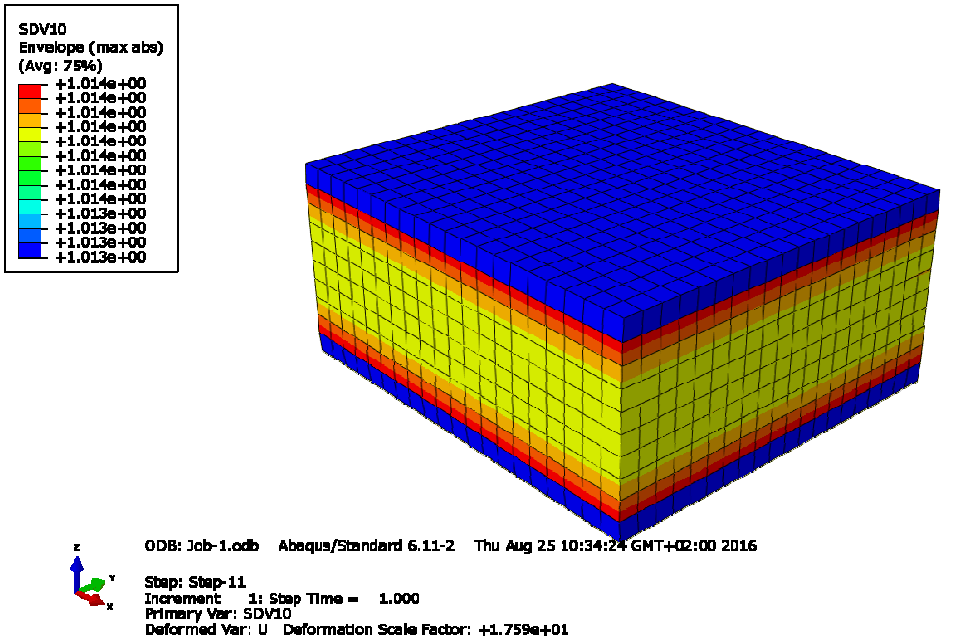

Figure 6-8 IFF for the end step with the possible contraction in the Z-direction

For σ_1 a small change in the range of values can be observed (cp. Table 6-7). The maximum values increased about 0,5%.

sigma_1 [MPa]			
Step nr	Abaqus (Z-no)	Abaqus (Z-yes)	Difference between max. Values [%]
1	0,1229-13,8	0,099-13,88	0,580
2	0,147-14,08	0,101-14,15	0,497
3	0,134-14,42	0,099-14,50	0,555
4	0,125-14,72	0,101-14,80	0,543
5	0,117-15,04	0,099-15,13	0,598
6	0,1145-15,36	0,101-15,45	0,586
7	0,114-15,67	0,099-15,76	0,574
8	0,1145-16,01	0,1-16,10	0,562
9	0,142-16,32	0,1-16,41	0,551
10	0,146-16,66	0,1-16,75	0,540
11	0,1145-16,98	0,1-17,07	0,530

Table 6-7 Sigma_1 comparison between two Abaqus models

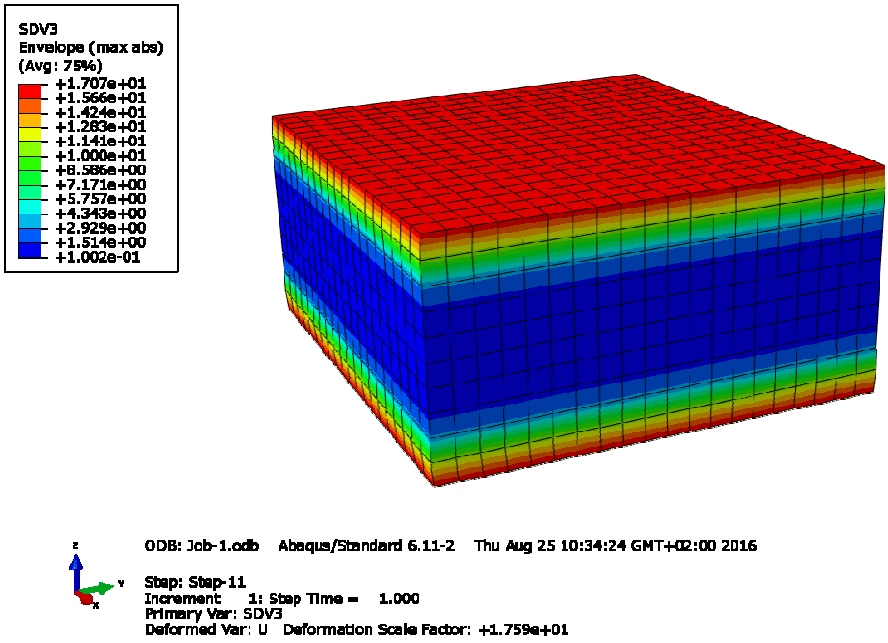

Figure 6-9 Sigma_1 for the end step with the possible contraction in the Z-direction

There is almost no difference in σ_2 between two models (cp. Table 6-8). Only in time step number 9 there is a difference in the range of stress values, but values in the middle of the layer are the same for both cases in this step.

sigma_2 [MPa]					
Step nr	Abaqus (Z-no)	Abaqus values in the middle of layer (Z-no)	Abaqus (Z-yes)	Abaqus values in the middle of layer (Z-yes)	Delta[%]
1	45,43-45,78	45,69	45,43-45,78	45,69	0
2	45,67-45,93	45,74	45,67-45,94	45,74	0
3	45,52-45,77	45,7	45,52-45,77	45,7	0
4	45,64-45,84	45,7	45,64-45,84	45,7	0
5	45,56-45,74	45,69	45,56-45,74	45,69	0
6	45,63-45,78	45,67	45,63-45,78	45,67	0
7	45,58-45,70	45,67	45,58-45,70	45,67	0
8	45,62-45,72	45,65	45,62-45,72	45,65	0
9	45,62-45,72	45,65	45,59-45,67	45,65	0
10	45,61-45,68	45,63	45,61-45,68	45,63	0
11	45,59-45,64	45,63	45,59-45,64	45,63	0

Table 6-8 Sigma_2 comparison between two Abaqus models

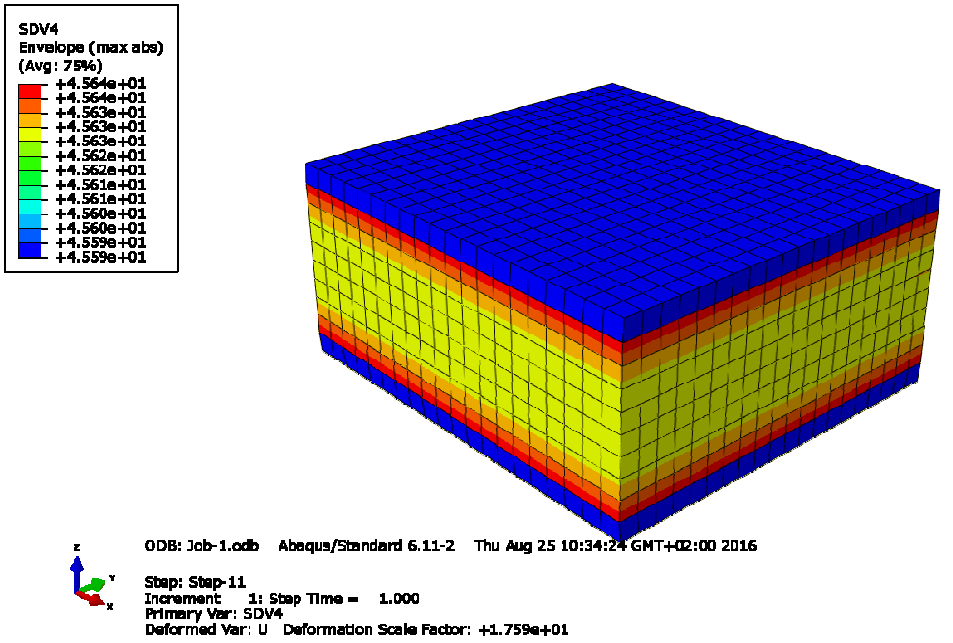

Figure 6-10 Sigma_2 for the end step with the possible contraction in the Z-direction

For Young's modulus, there are some small changes in the range of values in some time steps (cp. Table 6-9), but values in the middle of layer equivalent for every time step.

E_2 [MPa]					
Step nr	Abaqus (Z-no)	Abaqus values in the middle of layer (Z-no)	Abaqus (Z-yes)	Abaqus values in the middle of layer (Z-yes)	Delta[%]
1	9709-9842	9744	9711-9842	9744	0
2	9512-9533	9516	9512-9533	9516	0
3	9279-9391	9308	9280-9392	9308	0
4	9099-9133	9106	9099-9133	9106	0
5	8888-8984	8913	8889-8984	8913	0
6	8719-8762	8729	8720-8762	8729	0
7	8529-8613	8550	8530-8613	8550	0
8	8370-8418	8381	8370-8418	8381	0
9	8198-8272	8216	8199-8272	8216	0
10	8048-8099	8060	8048-8099	8060	0
11	7891-7958	7907	7892-7958	7907	0

Table 6-9 Young's modulus comparison between two Abaqus models

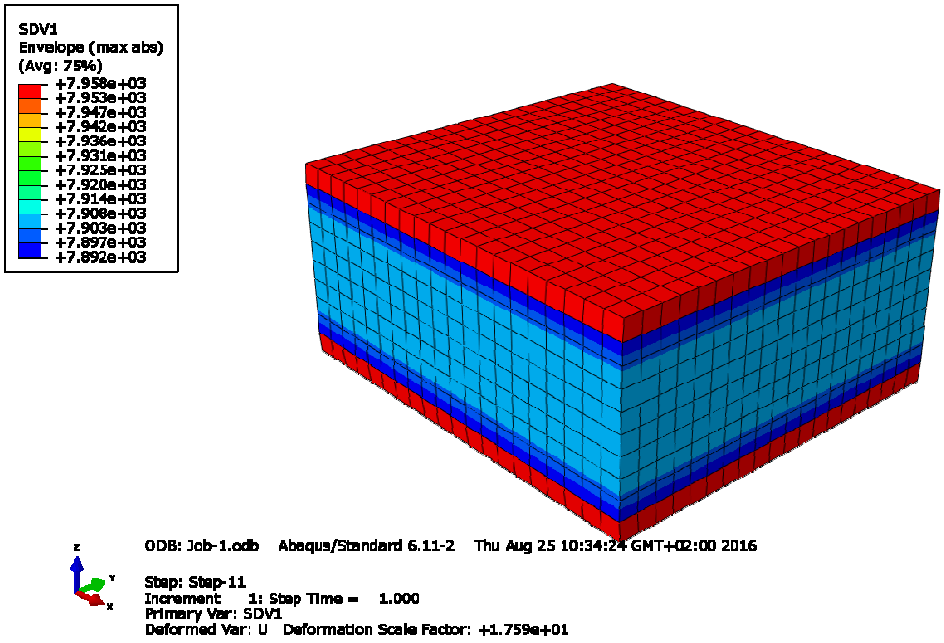

Figure 6-11 Young's modulus for the end step with the possible contraction in the Z-direction

For shear modulus, we cannot observe any changes (cp. 6-10).

G_12 [MPa]					
Step nr	Abaqus (Z-no)	Abaqus values in the middle of layer (Z-no)	Abaqus (Z-yes)	Abaqus values in the middle of layer (Z-yes)	Delta[%]
1	4937-4940	4938	4937-4940	4938	0
2	4933-4933	4933	4933-4933	4933	0
3	4928-4930	4928	4928-4930	4928	0
4	4924-4924	4924	4924-4924	4924	0
5	4919-4921	4920	4919-4921	4920	0
6	4915-4916	4915	4915-4916	4915	0
7	4911-4913	4911	4911-4913	4911	0
8	4907-4908	4907	4907-4908	4907	0
9	4903-4905	4903	4903-4905	4903	0
10	4899-4900	4900	4899-4900	4900	0
11	4895-4897	4896	4895-4897	4896	0

Table 6-10 Shear modulus comparison between two Abaqus models

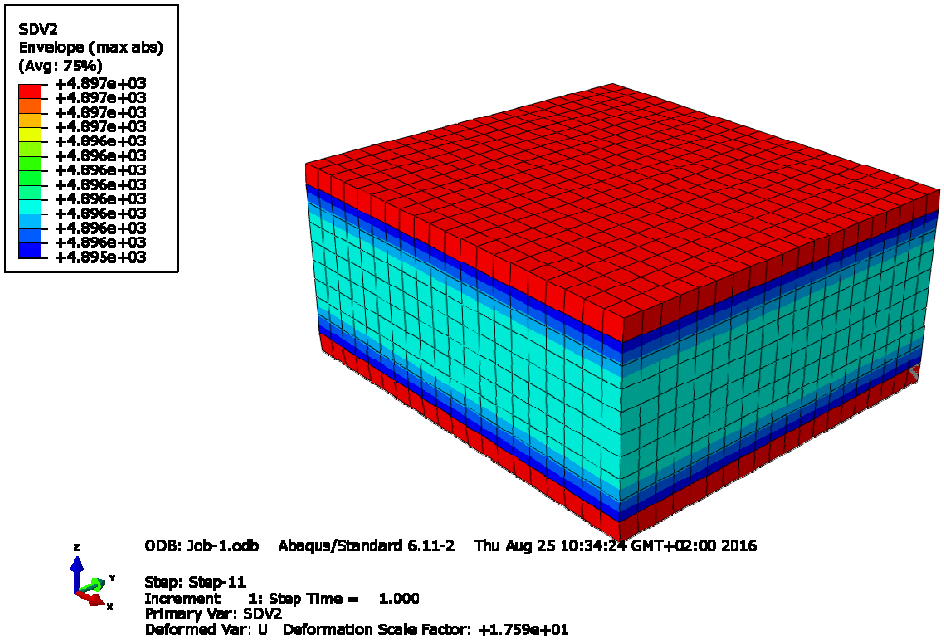

Figure 6-12 Shear modulus for the end step with the possible contraction in the Z-direction

Considering the results of the comparison between two Abaqus example, we can assume that the possible contraction in the Z direction does not influence meaningfully on the results in this particular example. Stresses σ_3, which appeared in the model are negligibly small (~10^{-4}) and they do not have huge impact on the IFF. More influence has the contraction in the Y direction. Nevertheless, it is shown that user-subroutine UMAT for Puck's criteria works for 3-dimensional state of stress. In this simple example there is now big difference between 2D and 3D state of stress but for more complex models the Compositor calculation will be not sufficient and the advantage of presented subroutine will be used.

7. Summary

In this thesis the action plane fracture criteria of Puck was succesfully implemented into Abaqus software. This process took a long time. At first, the action plane fracture criteria of Puck had to be considered and understand (cp. section 2.). We need to know what kind of information this criteria needs about state of stress and material constants. Then the whole process of lamina degradation in Abaqus was planned and discussed (cp. section 3). After considering what information must be provided by Abaqus to the subroutine and what information must be send back, a proper subroutine type was chosen to assure proper two way communication between Abaqus and subroutine. After that the subroutine was prepared in the Fortran code.

Prepared user-subroutine (UMAT) must have been validated. Do achieve a validation two example of degradation process were provided in Compositor (cp. section 4). There was the wish to compare both of them with the results from Abaqus. The validation was successful for the example showed in section 4.1. We achieve comparable results with the difference below 1% between values gained from Abaqus and Compositor. Unfortunately there was no possibility to compare the second example (cp. section 4-2) with the Abaqus. Nevertheless, it was shown that user-subroutine with Puck's criteria implementation is working and provides good results.

The big advantage of this subroutine is that it can be used for 3-dimensional model in Abaqus, for 3-dimensional state of stress. It was the main goal for this thesis and it was achieved. What is more the subroutine is easy to use does require advanced knowledge in Abaqus software.

Now the action plane fracture criteria of Puck can be used for more complex 3D models in Abaqus. The main reason that there was such a need to implement Puck's criteria into Abaqus is to develop researches about bended joints reinforced with yarns in the bending line and therefore improve their characteristics.

8. Conclusion

There is a few conclusion about this work. First of all, there is a need to create a proper model in Abaqus of a laminate when layers with different than 0° and 90° orientation of fibre occurs. There are some ideas proposed in section 6.3. These examples must be provide to check how implemented code is working when shear stresses appears.

Second thing that can improve implementation of Puck's criteria is to implement the tangent stiffness matrix instead of using secant stiffness matrix and change the procedure of looking for the solution. For examples provided in this thesis, using secant stiffness matrix and procedure showed in section 3, Fig. 3-5, is sufficient. Nevertheless, tangent stiffness matrix should be implement and it should be check which approach gives better solution.

In this thesis the implicit code was provided and we achieved good result with this method. However, even though implicit method is often more efficient for static problems, it is required to use explicit method when using Puck's failure criterion in numerical calculations of bonded repairs. This is due to the fact that failure is a highly dynamic process and only explicit method can produce the solution with the proper precision. That is why the next step should be transformation the code into explicit method.

As the last it this propose to find in literature an experimental example of failure in bended joints reinforced with yarns in the bending line. Then a proper model should be create in Abaqus and solution should compare with experimental data. It would be the last step of complex problem of the Puck's criteria validation. This thesis was the part of this process.

References

[1] H. Matthias Deuschle, 3D Failure Analysis of UD Fibre Reinforced Composites: Puck's Theory within FEA, Institute of Statics and Dynamics of Aerospace Structures Universit¨at Stuttgart,2010, ISBN 3-930683-99-7.

[2] VDI Guideline 2014, part 3: Development of FRP components (fibre reinforced plastics) Analysis, [in press].

[3] M.Knops, C.Bögle, Gradual failure in fibre/polymer laminates, RWTH Aachen University, 2005.

[4] Abaqus User Subroutines Reference Manual, Abaqus (3DS Dassault Systems, Paris, France)

[5] Chun H. Wang, Andrew J. Gunnion, On the design methodology of scarf repairs to composite laminates

[6] L. Lambrecht. Numerische Experimente zur Analyse der Einflussgr¨oßen auf die Degradation von mehrschichtigem GFK-Laminat. Master's thesis, Institut f¨ur Kunststoffverarbeitung (IKV), RWTH Aachen, 2003.

Appendixes

[1] Subroutine Fortran code: Puck_s_ criteria_UMAT.for

[2] Compositor degradation process of 3-layer lamina with 0⁰/90⁰/0° layers: T700_0_90_0_layup.xlsx

[3] Compositor degradation process of 3-layer lamina with -45⁰/90⁰/-45° layers: T700_45_90_45_layup.xlsx

[4] Material constants: material constants.xlsx

Declaration

Herewith I affirm that this master thesis is entirely my own work. Where use has been made of the work of others, it has been fully acknowledged and referenced.

Date Signature